The Use of Cryogenic Helium for Classical Turbulence: Promises and Hurdles

J. J. Niemela and K. R. Sreenivasan

The Abdus Salam International Centre for Theoretical Physics,
Strada Costiera 11, 34014 Trieste, Italy
E-mail: krs@ictp.trieste.it

Fluid turbulence is a paradigm for non-linear systems with many degrees of freedom and important in numerous applications. Because the analytical understanding of the equations of motion is poor, experiments and, lately, direct numerical simulations of the equations of motion, have been fundamental to making progress. In this vein, a concerted experimental effort has been made to take advantage of the unique properties of liquid and gaseous helium at low temperatures near or below the critical point. We discuss the promise and impact of results from recent helium experiments and identify the current technical barriers which can perhaps be removed by low temperature researchers. We focus mainly on classical flows that utilize helium above the lambda line, but touch on those aspects below that exhibit quasi-classical behavior.

KEY WORDS: cryogenic turbulence; thermal convection; quantized vorticies.

Table of Contents

1. INTRODUCTION

1.1. General Considerations

We cannot overstate the importance of turbulence in a wide range of contexts such as the motion of submarines, ships and aircraft, pollutant dispersion in the earth's atmosphere and oceans, heat and mass transport in engineering applications as well as geophysics and astrophysics.[1] Turbulence often occurs in conjunction with other features such as rotation, magnetic field and particulate matter,[2] so the knowledge of the subject is useful to a number of closely related problems such as interstellar dust and energy transport[3] and weather prediction and planetary magnetic fields.[4] The problem is also a paradigm for strongly non-linear systems, distinguished by strong fluctuations and strong coupling among a large

number of degrees of freedom,[5] and so even distant areas such as fracture[6]—perhaps even market fluctuations[7]—will benefit from a better understanding of turbulence. The subject is a particularly useful paradigm of a wide variety of non-equilibrium systems because the equations of motion are known exactly and can be simulated with precision. However, the complexity of the underlying equations has precluded much analytical progress, and the demands of computing power are such that routine simulations of large turbulent flows have not yet been possible.[8,9] Thus, the progress in the field has depended more on experimental input. This experimental input points in part to a search for optimal test fluids, and the development and utilization of novel instrumentation. The choice of low temperature helium as a test fluid is the subject of this review. We will examine how its use has impacted the field of turbulence and what obstacles there are in making further progress. Our view is that the use of low temperature helium yields several benefits, but its adaptation to the study of classical turbulence is not without impediments.

The review is organized as follows. In the rest of this section, we write down the fluid dynamical equations and show how the relevant non-dimensional control parameters emerge from them; these parameters allow us to unify the behavior of fluid systems under seemingly unrelated conditions. We will then discuss ways in which the use of low temperature helium can help address classical problems in turbulence. In section 2 we will also discuss some fundamental problems in classical turbulence and show how low-temperature fluids and techniques have been applied to address them. In section 3 we will discuss the main unresolved questions related to these efforts. Finally, in section 4 we will address the progress needed in order to better fulfill the promise of helium.

1.2. Fluid Equations and Non-dimensional Parameters

An accessible description of the equations of fluid motion, generally aimed at physicists, can be found in Tritton's book.[1] We will present a brief outline here. The equations are written down in a coordinate system that is fixed in space ("Eulerian" description). We will assume that continuum mechanics is a valid assumption for turbulence. Considering a fluid element of density ρ and moving at a velocity $\mathbf{u}$, the mass conservation takes the form

$$\frac{\partial \rho}{\partial t} + \nabla \cdot (\rho \mathbf{u}) = \mathbf{0}, \tag{1}$$

which, in the common case of constant density, reduces to the divergenceless condition

$$\nabla \cdot \mathbf{u} = \mathbf{0}. \tag{2}$$

For a Newtonian fluid, in which the stress and strain tensors are linearly related, the momentum equation reduces to

$$\frac{D\mathbf{u}}{Dt} = -\frac{1}{\rho}\nabla p + \nu\nabla^2\mathbf{u} + \mathbf{F}_{\text{ext}}, \tag{3}$$

in terms of the pressure p and kinematic viscosity $\nu = \mu/\rho$, where μ is the dynamic viscosity. For convenience of notation, we have used the so-called substantive or convective derivative $\frac{D}{Dt} = \frac{\partial}{\partial t} + \nabla \cdot \mathbf{u}$. The external body force term is represented by $\mathbf{F}_{\text{ext}}$.

The body force could arise from sources such as gravity, rotation and magnetic field. Of particular interest here is the gravitational buoyancy in thermally driven flows, for which there is only one component of the force in the direction of gravity and is given by $F_{\text{ext}} = g\alpha\Delta T$, where g is the acceleration of gravity, α is the isobaric coefficient of thermal expansion and ΔT is the temperature difference across a layer of fluid in the direction of gravity. It is customary to assume that the thermal driving does not affect pressure or the incompressibility condition, and that its major effect is to introduce buoyancy. This is the Oberbeck–Boussinesq, or simply Boussinesq, approximation.[10] The equation for energy conservation in the Boussinesq approximation (to be written as B-ap henceforth) is

$$\frac{\partial T}{\partial t} = \kappa\nabla^2 T - \mathbf{u} \cdot \nabla T. \tag{4}$$

Here κ is the thermal diffusivity of the fluid at temperature T.

Within the B-ap, Eqs. (2)–(4) describe the fluid motion and determine the velocity, pressure and temperature. These partial differential equations must, of course, be supplemented by the appropriate initial conditions and boundary conditions on rigid or "free" surfaces, conducting or insulating surfaces, rough or smooth surfaces, as appropriate. Under these conditions, the solutions of the equations of motion should indeed correspond to the observed flows, including turbulence. It is not always clear if small deviations from the ideal boundary conditions produce only small effects. We shall have more to say on this aspect in section 2.2.

We can economize our thinking by scaling all velocities in the problem by some characteristic velocity U and all lengths by some characteristic length L and time by L/U. (For time-dependent phenomena such as turbulence, the time has to be scaled independently but, given our limited purpose here, we shall not consider that situation explicitly.) The pressure p can be normalized by ρU^2. Then Eq. (3) for the case of simple pressure-driven flow can be written (now for normalized variables) as

$$\frac{\partial \mathbf{u}}{\partial t} + \mathbf{u} \cdot \nabla \mathbf{u} = -\nabla p + \frac{1}{Re} \nabla^2 \mathbf{u}, \tag{5}$$

where the so-called Reynolds number $Re = UL/\nu$ appears naturally as a consequence of the scaling of the variables. In the momentum equation in this form, we need not keep track of solutions of the problem in terms of various lengths and velocities of the flow and viscosities of the fluids separately, but simply in terms of various Re. The Reynolds number is a manifestation of dynamical similarity. That is, if we consider two flows that are geometrically similar, then they are *dynamically* identical if the corresponding Re is the same for both, regardless of the specific velocities, lengths and fluid viscosities involved. Matching such parameters between laboratory testing of a model and the actual full-scale object (the prototype) is the principle upon which aerodynamic model-testing is based. Physically, the Reynolds number is the ratio of the inertial forces (the term $\mathbf{u} \cdot \nabla \mathbf{u}$ in the substantive derivative, see Eq. (3)) and viscous forces (the term $\nu \nabla^2 \mathbf{u}$).

New similarity parameters can be formed depending on the types of external forces that need to be accounted for in Eq. (3). In thermal flows for which buoyancy plays a role, another dynamical similarity parameter, namely the Rayleigh number

$$Ra = g\alpha \Delta T L^3 / \nu \kappa, \tag{6}$$

emerges. Here g is the acceleration due to gravity, α, ν and κ are, respectively, the isobaric thermal expansion coefficient, the kinematic viscosity and thermal diffusivity of the fluid, and ΔT and L are the characteristic temperature difference and the length scale of the flow (which will be specified in later sections). Physically, the Rayleigh number measures the ratio of the rate of potential energy release due to buoyancy to the rate of its dissipation due to thermal and viscous diffusion.[11] The Prandtl number

$$Pr = \nu / \kappa \tag{7}$$

is the ratio of time scales due to thermal diffusion ($\tau_\theta = L^2/\kappa$) and momentum diffusion ($\tau_v = L^2/\nu$), and will be useful later on.

For the immediate discussion we will focus on isothermal flows driven by gradients in pressure. Turbulence in such systems is generated when inertia forces overwhelm the ability of the fluid to dissipate fluctuations directly, or when Re is large. Turbulence is made of fluctuations of many different scales (or "eddies") between the largest scale that is comparable to the size of the apparatus in which the flow is created and the smallest which is invariably damped out by viscosity. Eddies of a given characteristic length scale are associated with their own characteristic velocity and therefore their own characteristic Reynolds number. The large eddies are more energetic and

their Reynolds number is correspondingly large; by the principle of dynamical similarity, this can be considered equivalent to having a small viscosity. Thus, viscous effects are unimportant for large eddies and so their energy is not lost by viscosity; instead, the loss of energy occurs to other scales by the non-linear interaction with them. It is conventionally thought that the most effective interaction occurs with eddies of comparable sizes (though there is no rigorous proof that this is so). This gives rise to the notion of a cascade of energy from one scale of eddies to those of the neighboring scale. There is an average direction to the energy cascade because the energy is eventually dissipated in small scales. The Reynolds number for the small scales gets progressively smaller and so the viscous effects become important below a nominal scale; the smallest dynamically important scale is the one for which the Reynolds number is of the order unity. This is called the dissipation, or the Kolmogorov, scale, η.

As long as the energy is supplied steadily at a large scale ℓ, a statistically steady state is obtained; in this state, the most important dynamical phenomenon that occurs in the range of scales between the "large" and "small" scales—the so-called *inertial* range—is the scale-to-scale energy transfer without viscous dissipation. Energy is dissipated when it reaches the small scales; the rate of energy dissipation per unit mass, ϵ, is the same as the rate of energy input. (Thus, the energy dissipation rate, even if enabled ultimately by viscosity, does not depend on the magnitude of viscosity. Reducing viscosity simply allows the cascade to continue to even smaller scales until, as noted above, the characteristic Reynolds number of the smallest eddies becomes of the order unity.) The energy dissipation rate ϵ has the dimensions of cm^2 s^{-3} in cgs units and can be determined in order of magnitude from a dimensional analysis as proportional to u^3/ℓ, where u is a characteristic measure of the fluctuating velocity (such as its root-mean-square value) at the scale ℓ at which the energy is injected. This is the input power. Since the smallest scale η is responsive entirely to the viscosity and the energy dissipation rate, dimensional analysis shows that

$$\eta = (\nu^3/\epsilon)^{1/4} = \ell \mathrm{Re}_\ell^{-3/4}, \tag{8}$$

where $Re_\ell = u\ell/\nu$ is the characteristic Reynolds number of the large scale. For a fixed ℓ, the Kolmogorov scale becomes increasingly smaller as the Reynolds number increases. The corresponding time scale also becomes smaller. Thus, the spatial and temporal resolutions required of measurements become more demanding as the Reynolds number increases.

It is common to recast the energy dynamics in terms of a spectral language and discuss the nature of the energy spectrum $E(k)$, where k is

the wavenumber and $E(k)dk$ is the kinetic energy in the wavenumber shell between k and $k+dk$. Using the cascade picture of local interactions,[12] we can obtain

$$E(k) = C_k \epsilon^{2/3} k^{-5/3}, \tag{9}$$

where the proportionality constant C_k is empirically determined[13,14] to be about 1.5. Spectral decomposition is not particularly useful if the flow is confined or strongly inhomogeneous. A suitable wavelet decomposition with finite support is usually a better basis to use.

In the inertial range, which increases in size with Re_ℓ, we can expect the turbulent flow to be more or less homogeneous and isotropic. This is Kolmogorov's hypothesis of local isotropy.[12] *Self-similarity* in this range of scales means that turbulence at one length scale is similar to that at another length scale except for the change due to the scale ratio. That is to say, the local properties of the turbulence do not depend on the velocity and length scales of energy injection, and that at each scale the motion is the one *relative* to the immediate larger scales, which can be regarded as a steady background flow. If there are any universal statistical properties of turbulence in the inertial range, it is reasonable to look for them as $Re \to \infty$, since the separation between the energy-injection scales and the dissipative scales increases with Re—thus making it plausible to imagine that the inertial range would be independent of energy injection as well as dissipation. Needless to say, there are many practical questions of interest in engineering applications at high Reynolds numbers.

One goal of an experimentalist is thus to attain high enough values of Re. High enough Re means effectively any Re above the point at which certain scaling properties in the inertial range cease to vary. If high enough Reynolds numbers can indeed be attained using common fluids such as air or water, there is little sense in pushing the low temperature technology. This, however, is not the case in general. Another salient fact is that the increase in the Reynolds number is measured in terms of its logarithm,[15] and, in some respects, it makes sense to consider changes that may occur when Re changes by one or more decades. For this reason, a good experiment is one that permits Re to be explored over many decades—preferably in a single apparatus so we may neglect other effects such as changed boundary conditions, geometry and experimental protocol. As we will discuss in the next section, this possibility can be realized using helium as the test fluid.

1.3. The Promise of Low Temperature Helium as a Test Fluid

From this discussion, we may identify several aspects that must be considered in an experimental program: the generation of the desired

boundary conditions, similarity parameters that can be varied independently over a wide range, and the ability to make meaningful measurements, particularly when the Reynolds number is large.

1.3.1. Fluid Properties

Perhaps the principal promise of low temperature helium has been the recognition that its kinematic viscosity is low compared with any other fluid and much lower than that of the commonly used test fluids, air and water.

For comparison, Table I shows some typical values of kinematic viscosity for common test fluids. Helium has a substantial advantage in terms of viscosity over air and water, although these latter fluids are abundant and easier to use. One further point to be made especially is that helium II is similar to helium I in terms of the kinematic viscosity, here defined using the ratio of the normal shear viscosity to the total density. This remains true even to the absolute zero of temperature where an *effective* kinematic viscosity acts in turbulent flows even in the absence of a normal component of helium.[16]

Let us turn attention briefly to thermal turbulence and examine other beneficial properties of helium. Recall that the relations (6) and (7) define the two principal similarity parameters—the Rayleigh number Ra and the Prandtl number Pr—for systems in which buoyancy, derived from unstable heating, drives the flow. Ra is the primary control parameter and fully developed thermal turbulence occurs at very large values of Ra; again, we wish to produce flows in which Ra varies over a wide range. It is clear that the small kinematic viscosity of helium can make Ra also quite large. In addition, for helium gas, the thermal diffusivity $\kappa = k/\rho C_P$, where k is

TABLE I

Kinematic viscosities for some test fluids.

Fluid	T (K)	P (Bar)	ν (cm^2/s)
Air	293	1	0.15
Water	293	1	0.01
Helium I	2.2	SVP	1.8×10^{-4}
Helium II	1.8	SVP	8.9×10^{-5}
Helium gas	5.5	2.8	3.2×10^{-4}

Note: The numbers quoted for the liquid phases of helium are evaluated at the saturated vapor pressure (SVP).

the thermal conductivity of the fluid, ρ its density, and C_P is the constant pressure specific heat, is of the same order of ν (except near the critical point, where, in fact, it becomes vanishingly small because C_P diverges there). The Prandtl number $Pr = \nu/\kappa$ has a constant value near 0.7 sufficiently away from the critical point, as for air and other non-interacting gases, and increases rapidly only near the critical point.

The other fluid parameter which enters the definition of the Rayleigh number is the isobaric thermal expansion coefficient $\alpha \equiv -\rho^{-1}\partial\rho/\partial T$, where the derivative is evaluated at constant pressure. The sign of α determines the direction of the temperature gradient that is needed to induce buoyancy; since it is positive in most cases, the heating needs to be from below in order to destabilize the flow and set up turbulence. A notable exception is water for which the sign of α reverses below $4°$, as is also the case for liquid helium just above the lambda point.

For non-interacting gases, $\alpha = 1/T$, and so, low temperatures themselves have a particular advantage for buoyancy-driven flows. For helium near its critical point, α is thermodynamically related to the specific heat and also diverges. In summary, it is the combination $\alpha/\nu\kappa$ that determines the Rayleigh number, and we show it in Table II for helium, air and water.

One can use to advantage the enormously large values of the combination $\alpha/\nu\kappa$ near the critical point and generate large values of Ra. For illustration, if we consider a fluid layer some 10 m tall (difficult and expensive, but well within the capacity of presently available cryogenic capability) and a reasonable temperature difference of 0.5 K, Rayleigh numbers of the order 10^{21} are possible. Such large values are characteristic of turbulent convection in the Sun.[17]

TABLE II

Values of the combination of fluid properties $\alpha/\nu\kappa$ for air, water and helium.

Fluid	T (K)	P (Bar)	$\alpha/\nu\kappa$
Air	293	1	0.12
Water	293	1	14
Helium I	2.2	SVP	2.3×10^5
Helium II	1.8	SVP	—
Helium gas	5.25	2.36	6×10^9
Helium gas	4.4	2×10^{-4}	6×10^{-3}

1.3.2. Tunability and Scaling

It is also clear from Table II that at low pressures and temperatures sufficiently far away from the critical value values for $\alpha/\nu\kappa$ are quite small. In fact, the range shown in the table covers a factor of 10^{12}, so any given experiment of fixed size L can yield at least 12 decades of the control parameter Ra by this means alone. Further, if L is chosen to be large enough, this entire range of Ra can be shifted to a regime of developed turbulence where well-articulated scaling relations can be expected to occur. This is the motivation for the experiments to be discussed later.

It is worth noting that liquid helium at standard conditions of temperature and pressure can increase the range of Ra in a way that would be essentially impossible for air and water, but it does not have the same tunability as the gaseous state.

As mentioned earlier, of interest to turbulent convection is the logarithm[15] of Ra, and so several decades, rather than several factors of 2, of Ra are needed to extract accurate scaling information. One cannot simply increase the temperature difference to increase Ra if one were to maintain the closeness of fluid properties at the top and bottom of the convection apparatus. Cryogenic helium gas can, in fact, yield very high Ra while keeping ΔT relatively modest. Conventional fluids are not similarly flexible.

To see better how Ra can be varied over a wide range using cryogenic helium gas, it is instructive to rewrite Ra as

$$Ra = (\rho^2 \alpha C_P)\frac{g\Delta T L^3}{\mu k}. \tag{10}$$

The quantity in parentheses can be varied substantially and is the tuning parameter that allows the experiments to access large ranges and high values of Ra. For low densities and pressures (roughly $P < 1$ bar), we operate more or less in the non-interacting gas limit where both the expansion coefficient and specific heat remain essentially constant. Here, roughly, $Ra \propto \rho^2$ and by increasing the density by orders of magnitude (starting with a rarified state) we can generate a very wide range of Ra. Obviously, it is important to have a large value of L in order to push Ra to the high end.

Since part of the density dependence of Ra comes from the kinematic viscosity, a similar flexibility exists for flows governed solely by Re which is linearly proportional to the density.

1.3.3. Material Properties

An indirect benefit of the use of low temperature helium comes from the relation between the fluid properties and those of the solid material used to confine it. Boundary conditions play an important role in fluid mechanics and, in the case of thermal turbulence, the usual boundary condition at the horizontal surfaces is one of constant temperature. In practice, this condition is effected by using highly conductive plates with constant heating or with good temperature control. Annealed and oxygen-free copper has a thermal conductivity of order $1\,\mathrm{kW\,m^{-1}\,K^{-1}}$ to be compared with the nominal thermal conductivity of helium, which is of order 10^{-2} W $\mathrm{m^{-1}}$ K^{-1}.

Of course, the *effective* thermal conductivity of the fluid at very high Ra can be quite large because of turbulence and, at an Ra of about 10^{17}, be as high as 10,000 times that of the quiescent fluid. This brings the effective conductivity considerably closer to that of the plates and necessitates some correction. The correction[18] is negligible for helium except at the very highest Ra where it is of the order of a few percent; on the other hand, it could be of the order of 10-20% for conventional fluids even when the Ra is moderately high.[19]

1.3.4. "Table-top" Experiments

Let us now consider another experimental aspect that benefits from the use of low temperature helium: its size. Consider first the case for those turbulent flows in which $Re = UL/\nu$ is the principal similarity parameter, and for which the goal is to generate very high Re. The reader may have already wondered why Re could not be be made large enough by making either L or U (or both) large, and thus avoid the use of an uncommon and expensive fluid that is harder to work with than water or air. The first answer is the exorbitant cost and space constraints associated with large L. On the other hand, U has a more fundamental restriction. It cannot be arbitrarily increased without introducing compressibility effects, characterized by a new non-dimensional parameter, namely the Mach number (i.e., the ratio of flow velocity to the speed of sound in the medium).

We can illustrate the relative advantages of helium over air and water through a concrete example of pipe flow, spanning both laminar and fully turbulent conditions, for various magnitudes of surface roughness (which may become important at high Re depending on the diminishing height of the viscous boundary layer in comparison). The classical experiment is due to Nikuradse[20] from the 1930s. Nikuradse obtained turbulent

flow conditions with Re of up to 3×10^6. His apparatus used water and occupied two stories of a building. Recently, this range of Re has been duplicated in a standard dewar (13 cm diameter, 1.5 m tall) containing a pipe flow apparatus, where the pipe was only 5 mm in diameter.[21,22] This illustrates one of the compelling features of low temperature studies: that they are accessible to even modest sized academic laboratories.[a] Similarly, a 100 cm cross-section helium wind tunnel with feasible cooling power (of order 1 kW at the operating temperature) could match the Reynolds number of any wind tunnel in existence (usually tens of meters in its smallest dimension and hundreds of meters in the longer dimension).[17]

For thermal flows the situation is similar. From the definition of Ra, it is clear that it can be increased by going to larger and larger apparatus (because the characteristic length L appears as the third power in Ra). There are, of course, obvious limits to growth in this way. Furthermore, it is not always desirable to follow this route because each choice of L means a different apparatus with different conditions of roughness and other details which matter.[b] Increasing the temperature difference ΔT, as with U in the Reynolds number, has a fundamental limit: It cannot be made arbitrarily large since the fluid properties in Ra would be ill-defined over the sample across which a large temperature difference is imposed. Obviously, in the case of liquids one has to contend also with a phase change for too high ΔT. Related to this, as L becomes larger and larger for a fixed ΔT, temperature homogeneity in the boundaries becomes a practical issue at some point.

1.3.5. Other Promises

We mention in passing an area that has not received adequate attention but has been a primary motivator all along: the utilization of low temperature helium for model testing in aerodynamics and hydrodynamics. We mention at the end of this section an early experimental effort along this line.

In aerodynamic testing, one measures lift, drag and moments on a model and infers the corresponding values on the prototype. Since Re can often be very large in practical situations (of the order 10^8 or 10^9 for commercial aircraft or modern submarines),[17] it is difficult to match the

---

[a]It should *be* noted that pipe Reynolds numbers of the order 10^7 have recently been generated using air compressed to about two hundred atmospheres.[23] Highly compressed air has some advantages and some disadvantages compared to helium.

[b]In principle, there is a complementary problem in helium. A surface that could be regarded as smooth at low and moderate values of Re could become effectively rough at very large values of Re. For convection experiments even at the highest Ra, this does not seem to have been a problem.

prototype Reynolds number if the same fluid is used for model testing: L for the model is typically much smaller and there is not much maneuvering room on U without encountering technical problems of compressibility.[c] On the other hand, the very small kinematic viscosity of helium can compensate for the smaller L and U of the model, so that there is much potential in this area. Helium has an advantage over highly compressed air because the dynamic pressure $(1/2)\rho U^2$ is substantially smaller for a given Reynolds number, and hence the helium flow can be expected to exert significantly less force on the models (this being an issue of some practical importance). Another possibility here is the use of powerful superconducting magnetic balance and suspension systems both to orient models without the external arm or "stinger", and to measure forces on them.

One might suppose that results from testing facilities might be extrapolated to higher Re values of interest. Unless the flow configurations are clean, as is the boundary layer on a smooth horizontal plate immersed in a smooth stream, extrapolation over even a decade of Re is not accurate. Flows around practical objects include vortex shedding, interaction of vortices with solid surfaces, the production of acoustic energy, non-linear interaction among various parts of the flow, and so forth, so extrapolation could be misleading overall. Thus there remains a clear and compelling need for facilities that generate truly high Re. It suffices to say that there are not many opportunities to do full scale testing, other than perhaps at NASA Langley, where the cryogenic tunnel (the National Transonic Facility, or NTF) uses liquid nitrogen spray. The use of cryogenic helium instead of liquid nitrogen would be a natural extension of the idea behind NTF.

Briefly, we mention that testing of surface ships poses another critical problem: two important similarity parameters, Re, and the Froude number $Fr = U/(gL)^{1/2}$ which takes into account the effect of waves, cannot both be matched on a scale model using water, since U will have to be decreased to match Fr, which means that Re will be too small—typically by a few orders of magnitude. This could be avoided in principle by using liquid helium at a temperature and pressure for which the ratio of kinematic viscosities of helium and water can be chosen to compensate properly for the relative decrease in UL of the test model. (Note that ν does not appear in Fr.)

1.3.6. A Brief Historical Note

A small "superfluid wind tunnel" was constructed[24] in 1957 at Caltech with the idea of exploiting the superfluid properties of helium II.

---

[c]Note, however, that compressibility needs to be accommodated in testing transonic aircraft, and only the gas phase can in principle be utilized for a test fluid.

Although potential flow was observed (with no measurable lift on a pair of fly wings hanging in the tunnel) for low velocities, the inevitable appearance of quantized vortices altered that picture for higher flow speeds. The report of this early experiment acknowledged the participation of Feynman and Liepmann. Following some discussions on the subject, a proposal was made by Liepmann to construct a low temperature supersonic wind tunnel facility at Caltech,[25] but the project did not materialize; the needed technology development, including instrumentation, must have weighed heavily in the decision.

1.4. Alternatives to Laboratory Experiments

Before discussing the results from low temperature turbulence experiments, it is useful to consider the alternatives available to attain large values of the relevant control parameters such as Ra and Re.

First, it is reasonable to ask why nature's "laboratories", such as the atmosphere and oceans, cannot be instrumented and studied for turbulence dynamics. In fact, this is often done[26–28] but is not a substitute for controlled laboratory studies when questions become sharp and a deeper understanding is required.

The second comment concerns the role of direct numerical simulations (DNS) in which the appropriate equations are solved on a computer without making any approximation. This fine tool has been making tremendous progress with each generation of powerful computers, but still has a limited applicability for simulating practical flows at high Reynolds and Rayleigh numbers. The DNS efforts are hampered by the large number of degrees of freedom in turbulence that grows as $Re^{9/4}$. This can be easily seen from (8), where it is clear that the range of scales needing to be well resolved, ℓ/η, grows as $Re^{3/4}$. If the flow is to be followed in a numerical simulation with a uniform grid, the minimum number of necessary grid points (in three dimensions) is then proportional to $Re^{9/4}$. In fact, there is a recent theory[9] that suggests that this growth follows a steeper power of up to 3 instead of 9/4. Under certain circumstances, large eddy simulations (which compute only the large scales but model the small scales) and turbulence models (which compute only average information) do better in terms of providing useful information, but they are not satisfactory as universal recipes; the state of the art in computer hardware is years away from allowing us to address the most important problems in natural and engineering fluid turbulence.[8]

As in the quest to understand the limitations of the standard model in particle physics, we are compelled to push for the highest Re, not only for practical reasons, but also for bringing to bear more stringent tests of

existing phenomenology.[13,29] Thus, the prospect of modest-sized laboratories, primarily utilizing low temperature facilities, is quite alluring for the study of turbulence. This does not mean that all other facilities will be rendered obsolete, since not all unresolved questions concern very high Re or Ra.

2. MAJOR RESULTS IN HELIUM FLOWS

We will attempt to summarize major results in helium turbulence research but the review is not meant to be comprehensive. We will not address in detail turbulence in helium II about which another review has recently appeared,[16] but restrict attention to a "quasi-classical" result.

2.1. Hydrodynamic Turbulence

2.1.1. Kármán Flows

Here we discuss turbulence in the so-called von Kármán swirling flow between two counter-rotating disks immersed in a fluid, separated by a vertical distance H. Such flows typically generate intense turbulence. This increases the magnitude of the velocity scale and thus increases the Reynolds number somewhat, but the main feature that increases the Reynolds number is the use of cryogenic helium. As already remarked, the thinking in turbulence literature is that the rate of energy dissipation remains finite even as the viscosity vanishes.[30–33] Fundamental changes in the phenomenology of turbulence would result if this were not the case; for instance, the prevailing description of energy cascade through the inertial range of scales would have to be different. A convincing test of the existing phenomenology would require precise data at much higher Re, for which the turbulence is closer to a "universal" state (if one exists). A wide range of Re would be required to detect trends, if any. Naturally, to avoid complications due to changes in apparatus and measurement procedure, it is also desirable to extract this information from a single experiment. That helium is a viable working fluid for the purpose was recognized by Tabeling and co-workers. We now briefly describe the experiments carried out in that group using low temperature gaseous helium to measure turbulent energy dissipation at very high Re using the apparatus shown in Fig. 1.

The counter-rotating disks had a radius $R = 20$ cm. Additional radial "fins" were added to the plates to ensure stronger stirring of the fluid. The experiment was operated near 5 K with pressures ranging between about 2 bar and a few mbar. The Reynolds number, defined here as $Re = \Omega R^2/\nu$, where Ω is the angular velocity of the disks, varied from 10^4 to about
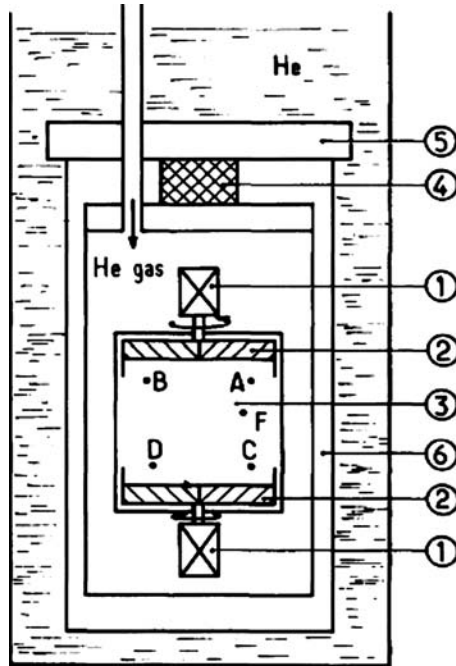
Fig. 1. Swirling flow apparatus. (1) dc motors. (2) Blades fixed on the rotating disks. (3) Working fluid. (4) Thermal link. (5) Copper plate. (6) vacuum. After Tabeling *et al.*[34]

10^7, the upper limit being roughly within a decade of characteristic atmospheric flows.

The quantity most often measured in these experiments is a component of the velocity in the direction of the disk rotation. This can be quite strong near the disks due to the entrainment of the fluid by the fins. It may be recalled that the hot-wire anemometry, which is a common tool for measuring turbulent velocities, requires the presence of a mean flow. Tabeling *et al.*[34] employed a version of the hot-wire (Fig. 2) to measure turbulence in their helium flow. In the usual fashion, such devices effectively measure the fluid velocity because of the forced convective cooling of the wire, which is held at a higher temperature than the ambient. The necessary calibration is done by comparing the average flow rates measured simultaneously by other means. Note that by virtue of their operational principle, hot-wires work best for nominally isothermal flow conditions; otherwise a more complicated calibration procedure must be used to separate the variations of ambient temperature. It is possible to alternately measure the background temperature signal from a nearby
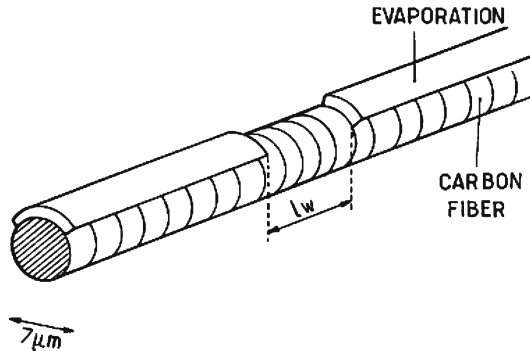
Fig. 2. Cryogenic hot wire probe, showing the active region, $\ell_w = O(7\ \mu m)$. After Tabeling *et al.*[34]

thermometer and apply the necessary corrections to the velocity signal from the hot wire. A more ambitious approach would be to operate a single wire in both the "hot" and "cold" (i.e., as a resistance thermometer) mode.

A time record of a velocity component obtained from a probe fixed in space is related partly to the temporal changes of the velocity at that point and partly to changes in the flow sweeping past the probe. In turbulence, the latter contribution far exceeds the former, so it is conventional to interpret fluctuations measured as a function of time entirely as spatial fluctuations, the connection being the sweeping by the mean velocity at the measurement point. This is the so-called Taylor's frozen-flow hypothesis: the underlying assumption is that the small scale turbulence is "frozen", or unchanging, for short times so that a variation of the velocity in time can be converted into a spatial variation by concurrent knowledge of a mean sweeping velocity. This hypothesis has limitations but is adequate for many purposes. (Significant advance in our understanding of turbulence may come from well-resolved measurements that are simultaneously functions of both time and space.) By this means, the wavenumber spectrum, $E(k)$, of velocity fluctuations, over the wavenumber k, can be obtained. The very high Reynolds number flows that can be created using helium possess large inertial ranges, thus making the scaling information more reliable. While hot-wire measurements at room temperature have been routine for some 60 years, this is not the case at low temperatures. First, any usable probe has to retain a large sensitivity at low temperatures. Second, because of the high Reynolds numbers in cryogenic flows, the corresponding Kolmogorov scale will be quite small in magnitude (of the order of $1\ \mu m$ in some of Tabeling's experiments) and the measurement transducers

must be correspondingly small. All this is non-trivial, but some success has occurred.

The hot wires used by Tabeling *et al.* consisted of carbon fibers $7\,\mu$m in diameter. To reduce the characteristic size along the length of the fiber, they were masked by another similar fiber stretched perpendicularly across, with a conductor (Au) evaporated on the remainder to provide a good electrical connection. The sensitivity of the carbon spot was within a factor of ten of that corresponding to a typical Allen Bradley resistor and so was still quite good. Thus the active area was a cylinder of diameter and length equal to $7\,\mu$m. Even this small size is much larger than the Kolmogorov scale at the highest Re achieved.

Figure 3 shows the probability density function (PDF) of longitudinal increments of velocity calculated on different scales. These increments are defined as

$$\Delta V_r = V(x+r) - V(x), \tag{11}$$

where V is the local velocity, and the separation length r is determined from the measured separation time using the Taylor frozen flow hypothesis. We can see from Fig. 3 that as the scales decrease toward the Kolmogorov dissipation length, the increments display more intermittency, indicated by the presence of long "tails" in the distribution. Intermittency refers to the existence of "patchiness" in the spatial distribution of small scales and leads a departure of the random velocity field from the self-similarity assumed by Kolmogorov's phenomenological theory. It is a general feature of turbulent flows related to the relatively frequent and large excursions of the data (e.g., velocity increments) from the mean; hence
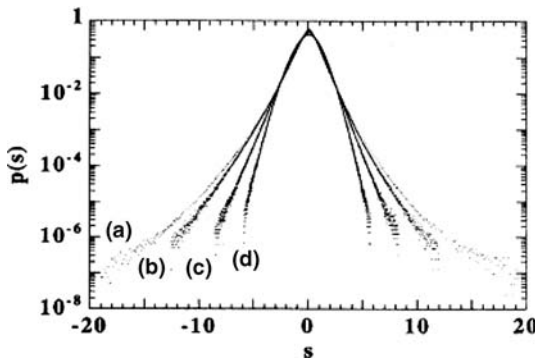

Fig. 3. Log-linear plot of the PDF of longitudinal velocity increments, calculated on different scales (a) $r \approx 10\mu$m. (b) $r \approx 100\mu$m. (c) $r \approx 1$ mm. (d) $r \approx 1$ cm. Here, $\eta \approx 2.5\mu$m and $R_\lambda \approx 3000$. The large-scale Reynolds number is of the order R_λ^2. After Tabeling *et al.*[34]

it appears in the form of stretched tails in the PDF. While there has been much effort in recent years to quantify and elucidate the nature of intermittency,[35,36] there is, as yet, no rigorous theory to explain all the observations. Intermittency renders Gaussianity inapplicable to turbulence broadly, though large-scale quantities do approximate Gaussian behavior under certain conditions (see Tennekes and Lumley).[37]

The intermittency as a relative measure of the distribution of tails can be partially quantified by the flatness factor given by

$$F(r) = \frac{<\Delta V_r^4>}{<\Delta V_r^2>^2}. \tag{12}$$

One can take the limit of this quantity as the separation distance approaches zero. This will yield the flatness factor $\tilde{F}$ of the derivative. Clearly, the authenticity of the derivative obtained from experimental data depends on whether the velocity has been resolved and sampled adequately. By "adequate", we mean that all spatial scales are resolved with good temporal fidelity. As already pointed out, there is increasing evidence that the resolution requirements become increasingly stringent with increasing Reynolds number[9] because smaller and smaller scales below the Kolmogorov scale are generated in that limit. In any case, even if we adopt the Kolmogorov scale as the standard, it is known from measurement that $\tilde{F}$ increases with increasing Reynolds number monotonically.[36] The data at higher Reynolds numbers have been obtained in the atmospheric flows where resolving Kolmogorov scale (of the order of 0.5 mm) from conventional hot wires presents no problem. One of the surprises from helium experiments (see Fig. 4) is that the flatness of the measured "derivative" decreases with increasing Reynolds number beyond a certain critical value, $R_\lambda \simeq 700$, where the Taylor scale Reynolds number R_λ is based on an internal scale of the flow (i.e., the Taylor microscale). The microscale Reynolds number is roughly equivalent to the square root of the Reynolds number based on the large scales which we introduced above. In fact, this break in behavior has been interpreted[39] in terms of a new bifurcation at around $R_\lambda \simeq 700$. If this is true, the measurements have revealed new physics that was missed earlier, or the derivative flatness is dependent on the particular method of generating turbulence, violating the spirit of scale similarity. The possibility that the tendency for the flatness to reach constancy at some high Reynolds number could be merely an experimental artifact related to the inadequate resolution of the probe (since the turbulent scales in the flow are small) was discussed[38] and regarded as unlikely. However, in another recent paper,[40] it has been pointed out that this anomalous tendency disappears when the resolution of measurement is improved. At the least, this debate suggests that there is a great need
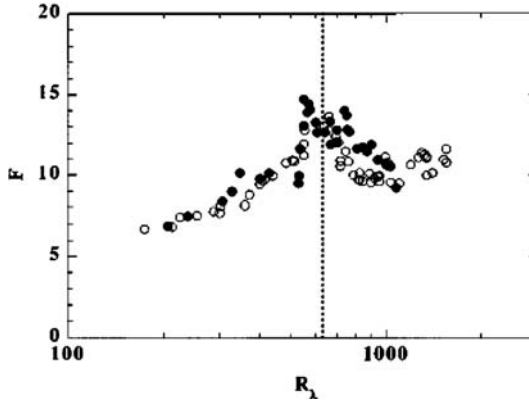
Fig. 4. Flatness of velocity derivatives versus R_λ (after Emsellem *et al.*[38]). The solid and open symbols refer to two different experimental cells, the larger one (open symbols) having a radius roughly 3 times that of the other (solid symbols).

to resolve the velocity data better in order to know with any certainty the true behavior of the flatness. We have already seen that there is an issue of probe resolution to be sorted out.

What might be the needed resolution? The conventional wisdom has been that the gradients can be computed from the velocity data reliably if the latter is measured with a resolution of the order of the Kolmogorov scale. That has been the ideal to aim for in most experimental efforts, and, indeed, some at high Reynolds numbers fall short of this goal. For some time, however, there has been a growing realization[9,41–43] that the Kolmogorov scale is a fluctuating quantity due to the (approximate) multifractality of the energy dissipation, and that scales significantly smaller than the mean value must exist. This feature has been verified (Schumacher *et al.* submitted) in which the grid resolution was much finer than the Kolmogorov scale. A recent paper[44] discusses how the grid-resolution depends on the moment order and the Reynolds number. The higher the order of the moment and the higher the Reynolds number, the more stringent is the required resolution in measurement and simulations. Simulations of passive scalar,[45] made with resolutions much smaller than the Batchelor scale (the nominally smallest scale for passive scalars), confirm that such finer scales indeed exist in quantities other than the velocity.

Finally, we note that similar experiments were conducted[46] using a pressure transducer in helium II flows in which hot wires would be ineffective. The output of these transducers could be related to the squared velocity and hence to the turbulent energy directly. At all temperatures below

the lambda point down to 1.4 K, the structure function exponents were indistinguishable from those observed in normal fluid turbulence. This was the best available direct evidence that turbulence in helium II could indeed behave quasi-classically. This issue has been discussed in another review,[16] and we shall comment on it section 2.3.

2.1.2. Free Jets

Another flow that is particularly well studied using water and air, and to whose study the use of low temperature helium gas can beneficially add, is the turbulent jet. Jets manifest as exhausts from combustion devices, environmental effluxes, materials processing problems, and in many technical devices. We will consider the case when the jet fluid is the same as the background medium into which it emerges and with which it eventually mixes. As in wakes behind solid objects, the turbulent fluid in jets is separated from the non-turbulent fluid by a relatively sharp and dynamically changing stochastic interface. The turbulent jet spreads into the background medium linearly with the distance downstream so that, on the average the flow takes the form of a cone.

In this system, the large-scale Reynolds number is based on the diameter of the orifice diameter and the exit velocity, and is given by

$$Re = \frac{U\ell}{\nu} = \frac{4\dot{m}}{\pi\ell\mu} \tag{13}$$

in terms of the mass flux $\dot{m}$ of a fluid with shear viscosity μ emerging from an orifice of diameter ℓ. In an experiment recently conducted at CERN, Re values of up to 10^7 have been achieved,[47] corresponding to flow rates up to $260\,g\,s^{-1}$. The apparatus used in this work is shown in Fig. 5. For comparison, the highest Reynolds number previously attained[48] is of the order 5×10^5, even though the latter facility was considerably larger. (A precise comparison is not very useful because it is not clear how the ancillary equipment, such as refrigeration in the case of cryogenic systems and the fluid pumping devices in the case of other fluids, should be compared in detail.)

Local velocity fluctuation measurements in the emerging jet were made using hot-wire anenometers[49] constructed by depositing a temperature sensitive resistive alloy (Au–Cr) on a small diameter (roughly 2–5 μm) glass fiber, exposed an active length of the fiber that was approximately equal to its diameter. Thus they are similar in design to those utilized earlier by Tabeling *et al.* (see Fig. 2) but employ a different thermometric material. The measured power spectral density, $E(k)$, is shown in Fig. 6a for two different Reynolds numbers, and displays the nominal $-5/3$ slope
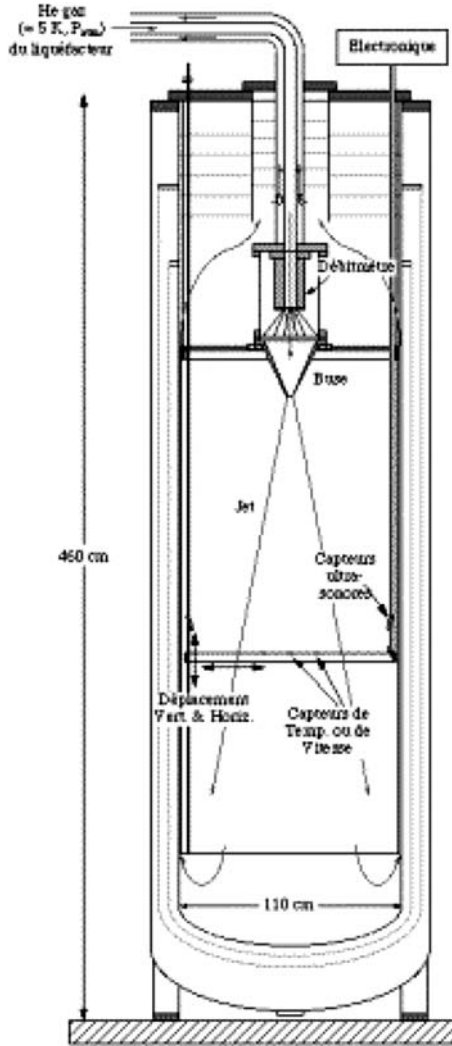
Fig. 5. Cryogenic helium gas jet apparatus at CERN. After Bézaguet *et al.*[47]

predicted by Kolmogorov.[12] Figure 6b shows the PDF of the velocity fluctuations for the highest Reynolds number and two different spatial increments δr, representing the two extremes of the inertial range in Fig. 6a. For the large scales the PDF is more or less Gaussian, while for small scales exponential tails are visible, indicative of small-scale intermittency
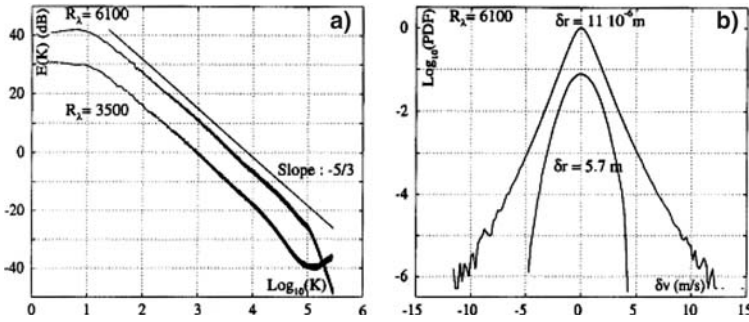
Fig. 6. (a) Power power spectra of the velocity fluctuations for $R_\lambda = 6700$ and 3500. The straight line has slope $-5/3$ and the abscissae is the wavenumber K in m^{-1}. (b) PDF of spatial velocity increments ($R_\lambda = 6700$) in semilog coordinates. The plot for larger δr has been shifted down one decade for clarity of display. Note the noise ceiling towards higher wavenumbers for $R_\lambda = 3500$ in (a) and the artificial manner by which the noise seems to have been filtered for the case $R_\lambda = 6700$. These wavenumbers are essential for proper dissipation estimates. After Bezaguet *et al.*[47]

as we saw in the previous section for the Kármán flow and which have been seen in other turbulent flows at high Reynolds numbers.[28]

The results so far are merely a guide-post to where one can proceed. The spectrum exhibits a sizeable inertial range and the maximum microscale Reynolds numbers exceed those typical of research wind tunnels and come close to those characteristic of geophysical turbulence.[26–28] Assuming that any universal traits of turbulence will be more likely revealed at very high Reynolds numbers, this cryogenic research is moving us in the right direction. The key accomplishment so far has been the development of facilities where high-*Re* flows are possible under well-controlled conditions. As new measurement procedures are developed, or existing ones improved, and as scientific questions become more refined, the existence of such facilities will assume greater importance for the advancement of the field. It is easy to see that the array of outstanding questions surrounds instrumentation.

2.2. Thermal Turbulence

We now turn attention to thermal convection, a subject in which the use of helium has played a major role in recent years. Turbulent thermal convection has long been a problem of major interest for a number of reasons: it plays a prominent role in the energy transport within stars, atmospheric and oceanic circulations, the generation of the earth's magnetic field, and countless engineering processes in which heat transport is

important. Threlfall[50] is credited with recognizing the advantages of using low temperature helium gas to investigate this problem in the laboratory. Later work by Libchaber and co-workers[51,52] brought a broader awareness of the potential of helium.

2.2.1. Rayleigh–Bénard Convection

We cannot hope to solve all real problems of convection and replicate in a laboratory every aspect related to complex boundary conditions, rotation, magnetic fields, ionization, chemical reactions, etc. Thus, it is generally agreed that it is better to make progress for a simpler problem that still contains the essential physics. In the case of buoyancy-driven turbulence, this paradigm is the Rayleigh–Bénard convection (RBC). In RBC, a thin fluid layer of infinite lateral extent is contained between two isothermal surfaces with the bottom surface maintained slightly hotter. When the expansion coefficient is positive (as is the case usually), an instability develops because the hot fluid from below rises to the top and the colder fluid from above sinks to the bottom. The applied driving force is measured in terms of a Rayleigh number, Ra, which is a non-dimensional measure of the imposed temperature difference across the fluid layer, see Eq. (6). The Prandtl number, Pr, defined in Eq. (7), is an additional dynamical parameter because it determines the state and thickness of the viscous and thermal boundary layers set up on the boundaries. With increasing Ra the dynamical state of RBC goes from a uniform and parallel roll pattern at the onset ($Ra \sim 10^3$) to a turbulent state at $Ra \sim 10^7$–10^8. (The onset value is independent of Pr but the turbulent state depends on it.)

For the low temperature experiments that will be discussed here we refer to the original papers for the exact set-ups,[53–55] but note the following salient features. To approximate the constant temperature top and bottom boundaries, annealed oxygen-free copper is used, with a conductivity near $1\,\mathrm{kW\,m^{-1}\,K^{-1}}$ at helium temperatures, nominally five orders of magnitude larger than the molecular conductivity of the contained helium gas. On the bottom plate a constant heating is applied, using a distributed heater (either a serpentine metal film or spiraling wires) while the heater at the top plate regulates the temperature as part of a feedback loop, where the plate is in contact with a cold reservoir (liquid helium bath) through an appropriate thermal resistance. Temperature fluctuations within the turbulent gas are measured using small cubes of doped germanium or silicon, nominally of the order of a few hundred microns on the side. The fluid is contained laterally by thin wall stainless steel, typically only as thick as necessary to withstand the pressure differential between the fluid

and the surrounding vacuum'; this minimizes parasitic heat inputs through conduction or convection. Radiative heat input through the vacuum is reduced through the use of shields at various graded temperatures.

The length scale associated with the lateral containment of the fluid introduces another dynamical parameter in the form of an aspect ratio $\Gamma = D/H$, where D is the diameter for the case of cylindrical containers and H, the vertical height between the top and bottom plates, is the relevant proxy for the length scale L in Eq. (6). For recent helium experiments, Γ is small of the order of unity, so the correspondence with theoretical models which banish lateral walls to infinity is fraught with difficulties. Considering that we wish to approximate $\Gamma \gg 1$, it is of some concern that most recent experiments have the value $\Gamma = 1/2$. It is, of course, easy to understand from the definition of the Rayleigh number in Eq. (6) why such a small aspect ratio has been chosen. Maximizing the height is paramount to achieving high Ra, and to make the width of the same order or much larger than the largest feasible height is often technically difficult *and* expensive. But the effects of small Γ are non-trivial; we shall revisit them subsequently.

2.2.2. Scaling

The heat transport in convection is usually given in terms of the Nusselt number Nu

$$Nu = \frac{q}{q_{\text{cond}}} = \frac{qH}{k_f \Delta T},\tag{14}$$

where q is the total heat flux, q_{cond} is the heat flux in the absence of convection, given by Fourier's law, and k_f is the thermal conductivity of the fluid. Nu represents the ratio of the effective turbulent thermal conductivity of the fluid to its molecular value and can reach values of over 10^4 in helium experiments[53] thus demonstrating the enormous enhancement of transport possible (one of the motivations for Threlfall's work[50]) in cryogenic turbulent convection. It is this global quantity that is often of interest in natural and engineering turbulent processes, and the ability to predict its value in the limit of high Ra corresponding to those processes—and often out of reach of laboratory experiments—is clearly useful. Since we normally expect $Nu = f(Ra, Pr, \Gamma, \ldots)$ to attain some limiting power-law form in fully developed turbulence as $Ra \to \infty$, we may hope to extrapolate results from experiments at the highest Ra if we have, indeed, exceeded the Ra beyond which the functional relation ceases to change.

In a simplistic view, it is possible to see two limiting cases for the scaling of Nu. In the first, we imagine that the global flux of heat is determined by processes occurring in the two thermal boundary layers at the top and bottom of the heated fluid layer. These layers, defined as the extent over which the molecular conduction remains important, are always present at the solid boundary where a heat flux is imposed, although they become thin at high Rayleigh numbers. Their thickness λ can be estimated as the distance over which the imposed temperature gradient would produce a state of marginal stability for convection; that is, when the Rayleigh number based on their height exceeds something of order 10^3. Assuming that the temperature outside the thermal boundary layer is uniform (because of turbulent mixing), one can easily show that $\lambda = H/2Nu$. Clearly, λ can become rather small; for instance, for the highest Ra achieved at present in the laboratory[53] the thermal boundary layers at the boundaries of a 1 meter column of fluid would have a thickness of the order $100\,\mu m$. In fact, this sharp temperature gradient realized in the limit of vanishingly small λ is the source of "stress" on the boundary layers and results in the emission of bursts of hot or cold fluid into the interior, commonly referred to as "plumes" or "thermals".[56,51,57,58]

Now, in the sense that the bulk fluid outside the boundary layers is fully turbulent and "randomized", it acts more or less as a thermal short circuit. Therefore its precise nature or spatial extent is immaterial to the flux of heat and from the definition of Nu given in (14) we can then immediately write down the asymptotic power law[59] as $Nu \sim Ra^{1/3}$, where we assume that the heat flux q appearing in Nu has no implicit height dependence (no internal energy sources). This simple argument has been made more precise by others[60] and rigorously shown[61] to hold when Pr and Ra are both very large.

There is another limit one can think of in which molecular properties lose relevance in determining heat transport—for instance, when boundary layers are mixed by a vigorous turbulent flow so that molecular conduction is supplanted entirely by small scale turbulent motion. Here, an exponent of 1/2 (modulo logarithmic corrections) has been proposed; the phenomenological theory has been developed by Kraichnan[62] and later shown to be relevant when boundary layers are artificially removed from the problem.[63] The theory of Grossmann and Lohse[64] is consistent with both "asymptotic" scalings given above, in different regimes of Ra and Pr, but does not anticipate the 1/2-power to occur in the range covered by most available experiments. The one experiment[53] where it could perhaps have been expected to appear does not show it. In Kraichnan's work[62] this scaling was proposed to occur for $Ra \sim 10^{24}$. Of course, it is not merely the exponent, but also the prefactor which determines our ability to make
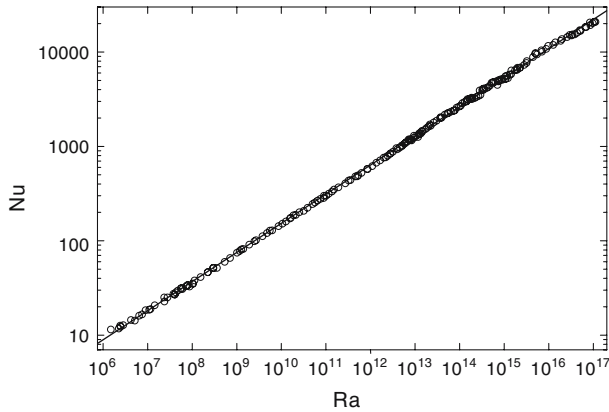
Fig. 7. Log-log plot of the Nusselt number versus Rayleigh number. The line through the data is a least–square fit over the entire Ra range, and represents a $d \log Nu/d \log Ra$ slope of 0.32.

a prediction of Nu at higher Ra, so it is of some importance to determine both from an experiment at *sufficiently* high Ra. To get these numbers accurately, for technical reasons (see below), a few more decades of Ra will be required. As we saw in the introduction, low temperature helium gas provides an opportunity not only to attain the highest possible Ra in an apparatus of given height, but also to obtain many orders of magnitude of it without making mechanical changes to the apparatus (or change its aspect ratio which is often done in conventional fluids).

Figure 7, plotted using the data from Niemela *et al.*,[53] illustrates the enormous range of Ra and Nu possible in low temperature experiments of modest size. We show this figure mainly because it represents the highest Ra achieved in a laboratory and also the largest range of Ra in the turbulent scaling regime, both of which represent the fulfilment of the promise of cryogenic helium gas. The average slope over 11 decades is 0.32, close to 1/3. Low temperature experiments of Chavanne *et al.*,[54] and by the present authors for a different aspect ratio,[55, 65] have found a scaling exponent close to 1/2 over a limited range at the very highest Ra, but those high-Ra data have been obtained very close to the critical point of helium. The interpretation in this case is complicated because the data cover the region of large departures from Boussinesq conditions and variable Prandtl number (remember that increasing Prandtl number serves to stabilize and laminarize the boundary layers, in contrast to the conditions prescribed for observing the 1/2 scaling).

The data shown in Fig. 7 have been corrected for two main effects, although the corrections for these low temperature experiments are rather small. We have already pointed out the thermal advantages of cryogenic helium experiments over conventional fluid experiments in having heating plates of thermal conductivity many orders of magnitude greater than that of the fluid. However, for very high Ra, the effective thermal conductivity of the fluid, $Nu \times k_f$, becomes large, and the plates can no longer be regarded as strictly isothermal. The resulting "mixed" boundary conditions could then affect dynamical features such as plume production.[18] This effect is unmeasurably small over almost the entire range of Ra used by Niemela et al.[53] For the data shown in Fig. 7, we estimate the corrections to be order of a few percent only for $Ra > 5 \times 10^{16}$. The same order of magnitude correction in similarly constructed water experiments would develop at a Rayleigh number roughly seven orders of magnitude lower!

The other correction required is that due to sidewall conduction. Some (small) part of the heat is inevitably conducted from the bottom plate to the top through the side walls. The standard procedure is to subtract this parallel conductance, assuming for this purpose that the temperature difference prescribed between the plates varies linearly between them. The onset of turbulence and thermal short-circuiting in the bulk of the flow makes such corrections inadequate in a range of moderately large Nu, where the temperature profile is no longer approximately linear, but Nu not so high as to make any parallel conduction negligible. Various models[55,66–69] have been developed for the purpose, all of them reasonable but none perfect. The data in Fig. 7 have been corrected for plate effects using the scheme proposed by Verzicco[18] and modified in Brown et al.[19] and for wall effects using the scheme proposed by Roche et al.[66]

Another area worth mentioning is the detailed study of a weakly organized, coherent mean wind[70–76], adding significantly to our overall understanding of turbulent convection. The wind phenomenon has had a rather broad reach; for example, quantitative observations of occasional reversals of the mean wind flow direction have been shown using data obtained from helium experiments[77,78] to be related to standard critical systems. Furthermore, the lifetimes of the metastable states of the bi-directional mean flow have intriguing analogies with reversals of the earth's magnetic field polarity, a phenomena arising from turbulent convection within the outer core;[4] there is also a more quantitative statistical analogy with the lifetime of solar flare activity driven by turbulent convection in the Sun's outer layer.[79] This latter conclusion may indicate the existence of an underlying universality class, or a more direct physical similarity in the convective processes that lead to re-shuffling of the magnetic

footprints and ultimately to flare extinction. In general, the understanding of the transition from one metastable state to another is an unexplored territory in the presence of large fluctuations.

Finally, we briefly mention the contributions from low temperature convection experiments[80] on the effect of rough surfaces[81] on the global heat transport in turbulent convection. A principal motivation in the low temperature studies was to illuminate the nature of a proposed "ultimate regime". Indeed, the heat transport increased with a slope of about 1/2 above the roughness transition[81] (defined as the Rayleigh number at which the thermal boundary layer thickness becomes of order the size of the roughness elements). Unfortunately, the roughness transition occurred within a decade of the highest possible Ra: from Du & Tong,[81] it is known that the heat transport is increased by up to 40% when the roughness transition has been crossed due to the extra transmission of thermal plumes from the roughness tips, and some ambiguity arises as to whether the increased heat transport slope represents a change of slope or is simply a transition between parallel curves displaced by some 40%. Because it has been difficult to obtain all the flow details in low temperature experiments, such possibilities have not been answered. At the least, one needs to repeat the experiment with larger roughness elements so that the roughness transition occurs at much smaller Ra. This poses an attractive challenge for further work.

2.3. Superfluid Turbulence

Several "classical" experiments have been performed in liquid helium below the lambda temperature. These experiments also can be interpreted in a quasi-classical sense, which is what will be done below. In many cases, this correspondence cannot be made because it depends on factors such as the ratio of normal to superfluid densities, or whether, say, the normal fluid remains at rest in response to the driving.[16, 82–84]

2.3.1. Grid Flows

The canonical method of creating a nearly isotropic and homogeneous turbulent flow is to force a fluid through a grid of crossed bars, usually by placing a stationary grid in a stream of air or water in a wind or water tunnel. Alternatively, one can tow a grid through a stationary body of fluid. Several such experiments in water exist. The relevant references, as well as recent measurements in helium I, are reported in White et al.[85] A series of measurements have also been made in which a grid is towed through a stationary sample of helium II, contained within a square

channel of $1\,\text{cm}^2$ cross-section.[86–89] In recent experiments,[89] there were 13 meshes across the channel, this number being comparable to that commonly used in wind tunnels. The grid velocity in all cases was approximately $V_g \le 2.5$ m s^{-1}. The mesh Reynolds number defined as $Re_\text{M} = v_g M\rho/\mu$, where μ is the dynamic viscosity of the normal fluid and ρ the total density of the fluid, varied between 5000 and 200,000. (The total density ρ is the sum of the superfluid density ρ_s and the normal fluid density ρ_n.) These mesh Reynolds numbers must be considered quite large given the compactness of the apparatus. There is some lack of clarity as to which density must be used below the lambda temperature. The present choice seems plausible because, when the superfluid vortex tangle becomes polarized and the superfluid and normal fluid velocity fields are correlated, helium II should behave as a single fluid with the combined density ρ for scales large compared with the average inter-vortex line spacing.[90] In fact, the effective kinematic viscosity of turbulent grid flows in helium II has been shown to be proportional to the quantum of circulation, κ, which has the same units without an explicit density dependence. Both κ and ν defined above have similar magnitudes but this is regarded as a numerical accident.[16]

For various values of Re_M, observations were made of the decay of the quantized vortex line density in the measuring volume following the upward pull of the grid. The velocity V_g was constant from well below the measuring volume to well above it.[91] On the opposing walls of the channel two second-sound transducers were situated, using flush-mounted vibrating superleaks. In this case the channel acted as a second sound resonator. The best results were typically obtained using a high harmonic of the fundamental, corresponding to 25–40 kHz.

The length of quantized vortex line per unit volume, L, can be deduced from second sound measurements through the relation

$$L = \frac{16\Delta_0}{B\kappa}\left(\frac{A_0}{A} - 1\right),\tag{15}$$

where A and A_0 are, respectively, the amplitudes of the second sound standing wave resonance with and without the vortices present, Δ_0 is the width of the resonance curve at half maximum of the second sound resonance peak in the absence of vortices, B is the (frequency-dependent) mutual friction constant.[92] A more general formula[88] is

$$L = \frac{8u_2}{\pi B\kappa d}\ln\left[\frac{1 + p^2 P + \sqrt{2p^2 P + p^4 P^2}}{1 + P + \sqrt{2P + P^2}}\right],\tag{16}$$
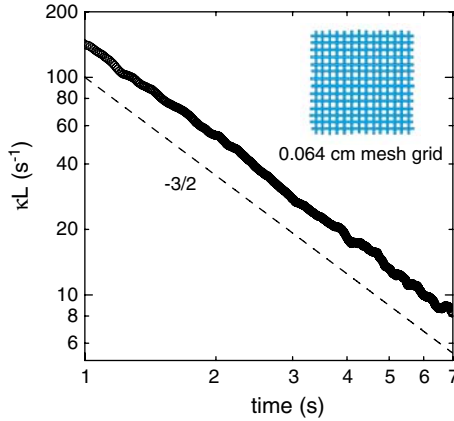
Fig. 8. The log–log plot of the decaying vortex line density versus time obtained with a conventional grid. The data correspond to $Re_M = 1.5 \times 10^5$ and a temperature 1.5 K. The grid passed the measurement volume at $t = 0$, and precisely that part of the decay data used for determining the effective kinematic viscosity of the turbulence (see text) is shown here. The exponent $-3/2$ is shown by the displaced dashed line. A schematic of the grid used to generate these data is shown in the inset.

where $p = A_0/A$ and $P = 1 - \cos(2\pi d\Delta_0/u_2)$, u_2 the second sound velocity and d the channel width. The final resting position of the grid following the pull-through was against the top wall of the channel, with a constant translating force applied to compensate for the effects of expansion on the part of the pulling rod that is in contact with room temperature. Otherwise, the small and variable displacement downwards of the grid would affect the second sound resonance properties of the channel during decay.

An example of decaying line density is shown in Fig. 8 for the temperature of 1.5 K in the region of power-law decay. Similar data were obtained for other temperatures as well. The time-dependent line density was spatially averaged over the measurement volume of order $d^3 \cong 1\,\mathrm{cm}^3$. The slope of $-3/2$ is precisely what one might expect if the superfluid turbulence behaved like classical turbulence,[16,93–96] except at the smallest scales where the precise mechanism of energy dissipation determines turbulence characteristics. The relevant notion is that the vorticity fields of the classical and quantized turbulence are coupled to each other.[17,97]

We shall now state the underlying assumptions concretely. First, we note that the turbulent energy dissipation rate per unit mass, ϵ, is not a small scale property but one that is inherited from the large scales at which energy is injected into turbulence. For classical homogeneous turbulence, ϵ is exactly equal to kinematic viscosity times the mean squared

vorticity. For decaying grid turbulence in helium II, we may *assume*[95,16] that the total energy dissipation per unit mass in the turbulent fluid is analogously given by

$$\epsilon = \nu' \kappa^2 L^2, \tag{17}$$

where ν' is a proportionality constant with units of kinematic viscosity.

Second, as already mentioned in section 1.2, the energy dissipation rate in fully developed turbulence is thought to be independent of viscosity, so that

$$\epsilon = C_\epsilon u^3 / \ell, \tag{18}$$

where C_ϵ is a constant for sufficiently large Reynolds number,[31–33,98] in practice for $R_\lambda > 100$. Here, u can be taken as the root-mean-square value of the turbulent velocity. The precise value of C_ϵ depends on the definition[31,32] used for ℓ and is about 0.5 for the definition employed here. We assume that this type of relation holds for helium turbulence as well.

Third, we assume that the length scale ℓ grows with time just as in classical turbulence. If this is true, at late stages of decay, it will become comparable to the channel width d and will cease to grow further. Of course, it does not prevent the length scale from growing in the direction of the grid motion, thus rendering turbulence anisotropic, but we shall not consider this possibility. If ℓ is a constant, the above relation becomes

$$u^2 = \left[\frac{\epsilon d}{C_\epsilon}\right]^{2/3}. \tag{19}$$

Noting further that $d/dt\,(\frac{3}{2}u^2) = -\epsilon$, we have

$$-\epsilon \left(\frac{d}{C_\epsilon}\right)^{2/3} = \epsilon^{-1/3}\frac{d\epsilon}{dt}. \tag{20}$$

Integrating and using (17) we have

$$\kappa L = \left[\frac{27}{\nu'}\right]^{1/2} \frac{d}{C_\epsilon} t^{-3/2}. \tag{21}$$

With $C_\epsilon \simeq 0.5$, this relation turns out to be identical to that derived by Vinen & Niemela[16] using a somewhat different argument. The $-3/2$ decay of the line density follows from Eq. (17) relating the line density to the energy dissipation rate per unit mass. We note that it does not depend directly on the form of the Kolmogorov $-5/3$ energy spectrum, but rather, more generally, from the finiteness of the energy dissipation expressed in (18).
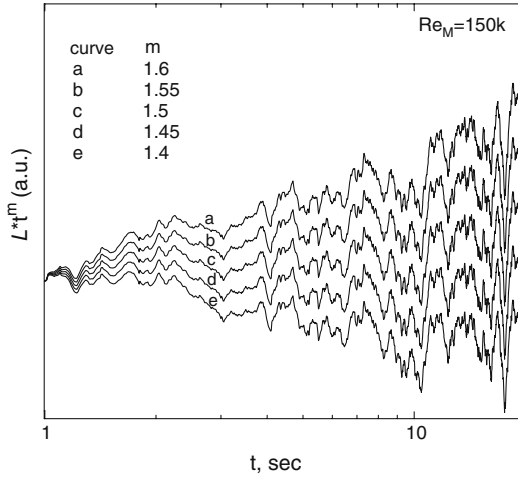
Fig. 9. Plot of the line density normalized by t^m where the exponent m takes on the values (a) 1.6, (b) 1.55, (c) 1.5, (d) 1.45, (e) 1.4. Clearly, the curve labeled "c", representing the exponent 1.5, gives the best results. (i.e., is most constant in t).

In Eq. (21), the only explicit unknown is ν'. We may find it by fitting (21) to the decay data for $L(t)$ in the power-law part of the decay (see Fig. 8). There is, in fact, some uncertainty due to ambiguities in the value of the frequency-dependent mutual friction coefficient used to determine the vortex line density, as well as the $-3/2$ exponent forced in the fitting procedure. The latter concern is not too strong, as illustrated in Fig. 9, where we have normalized the data represented in Fig. 8 by the value of time raised to an exponent that varies around 1.5 in gradations of 0.05. We see that $-3/2$ is indeed the best exponent. Finally, the values of ν' obtained according to the prescription given above are shown in Fig. 10.

The deduced values of the effective kinematic viscosity are of the same order as the kinematic viscosity based on the total fluid density, but the details are somewhat complex. An analysis of the energy decay within the two-fluid model[16] found that indeed the relation for the energy dissipation rate per unit mass given in Eq. (17) applies to helium II, but with ν' proportional to the quantum of circulation κ and independent of normal fluid viscosity. The predicted value of ν' is also shown in Fig. 10 and it can be seen that there is good agreement for much of the temperature range. However, as noted previously[16] the calculation does not produce the leveling off of ν', indicating that more work is needed.

In this context, we point out that a recent grid experiment due to Bradley et al.,[99] in which the working fluid was superfluid ^{3}He–B, finds a similar
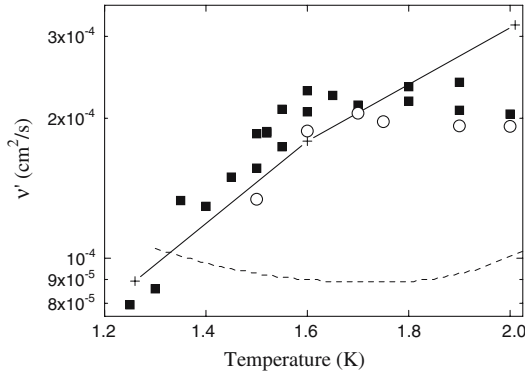
Fig. 10. The effective kinematic viscosity of the superfluid turbulence ν' deduced from vorticity decay data at various temperatures. The dashed line represents $\nu = \eta/\rho$, where η is the normal fluid viscosity and ρ is the total density of helium II. The squares represent the kinematic viscosity deduced from decay data obtained using an older grid,[86,88] while the open circles represent the present data. The pluses connected by the solid line represent a model calculation for the effective kinematic viscosity[16] which is proportional to the quantum of circulation, a quantity that has the same units and approximately the same numerical value as the kinematic viscosity based on the normal fluid viscosity and the total fluid density.

decay as discussed above, although in their case the grid was vibrated rather than pulled through the fluid. For ^{3}He–B, the normal fluid is sufficiently viscous that under normal forcing conditions it cannot be made turbulent. At low enough temperatures where the mutual friction is weak, turbulence can exist in the superfluid[83] irrespective of the behavior of the normal fluid. At the lowest temperatures of the experiments of Bradley *et al.* the normal fluid fraction is negligibly small so that the turbulence observed occurs in what might be then regarded as pure superfluid, where classical decay mechanisms cannot operate. The interesting observation of these experiments is that a similar decay occurs as in the experiments towing a grid in ^{4}He (see Fig. 8), but the decay can only be quantitatively reconciled if the effective kinematic viscosity is taken to be proportional to the quantum of circulation as illustrated in the case of ^{4}He in Fig. 10. Since there is no possibility of a "numerical accident" as in the case of ^{4}He, where $\eta_n/\rho \sim \kappa$, these experiments support the notion of an effective kinematic viscosity that does not depend of the normal fluid viscosity.[16]

2.3.2. Superfluid Kármán Flows

A more direct examination of quasi-classical behavior in superfluids was carried out by the Kármán flow experiments below the lambda
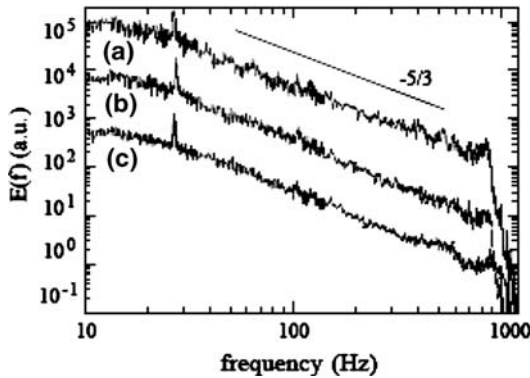
Fig. 11. Results by Maurer & Tabeling[100] showing the energy spectrum obtained under the same conditions but at different temperatures (a) 2.3 K, (b) 2.08 K, (c) 1.4 K.

point.[34] In these experiments the Kolmogorov spectrum was found to work equally well to describe the distribution of turbulence energy. In fact, it was impossible to distinguish which measurements were taken above or below the superfluid transition, all giving the $-5/3$ law decay in the energy spectrum Eq. (9). Measurements were made using a local pressure probe inserted into the fluid in a region close to the rotating plates and thus having a large mean flow. The pressure fluctuations measured by the probe were then interpreted to give the velocity fluctuations which are directly connected to the turbulent energy.[100] The resulting energy spectra in frequency space are shown in Fig. 11. Note that the three curves are displaced for clarity, and only the curve labeled "A" is taken for a temperature above the superfluid transition. Of the other two, the curve labeled "C" was measured at 1.4 K, where the normal fluid fraction of the density is only a few percent, yet all three instances show essentially identical energy spectra (with the canonical $-5/3$ roll-off). At all temperatures below the superfluid transition, the structure function exponents, for example, were identical to those observed in normal fluid turbulence.

We add the final note that all the cases considered here are essentially "table-top" experiments.

3. SOME UNRESOLVED ISSUES

3.1. Hydrodynamic Turbulence

As we saw, very large values as well as large ranges of Re were possible in the Kármán flow using gaseous helium. A transition to reduced

intermittency was noted above a certain threshold Re. This has not yet been seen in turbulence work using water and air. It is not firmly established that the observed result is due to poor probe resolution, but there are enough concerns on this score that the result will need to be substantiated by measurements in other flow configurations by using different or smaller probes. There are questions on how to assess the errors due to the finite size of the probe. If the local Re based on the probe size is large enough, we have to worry about vortex shedding by the probe itself, leading to altered heat transfer laws for the hot wires.[101] Analysis of this behavior[38, 102] shows that hot wire response would likely affect flatness measurements: the viscous boundary layer set up around the probe limits the response time by the need for heat to diffuse through this layer and maintain the temperature of the probe constant.[102]

3.2. Thermal Turbulence

As noted in section 2.2, very near the critical point, the increase in Ra is associated with the divergence of the specific heat. The diminishing value of thermal diffusivity makes the Prandtl number grow substantially in excess of 0.7. Thus, two control parameters are simultaneously varying. This effect begins for $Ra > 10^{13}$ in the experiments of Niemela *et al.*[53] and for $Ra > 10^{10}$ in the experiments of Chavanne *et al.*[54]

Additionally, close to the critical point, the temperature dependence of the fluid properties can lead to large enough vertical asymmetry for the applicability of B-ap to be in serious doubt. Unfortunately, little is known about such departures from B-ap at high Ra, and we have to appeal with meagre justification to practices that are common in the work near the onset of convection. For instance, the common practice near the onset is to evaluate all physical properties of the fluid at the midplane temperature, but it has become clear that this practice cannot be justified in the turbulent regime, especially as one operates near the critical point of helium.

One suitable measure of Boussinesq conditions is given by the fractional change in density across the layer

$$\frac{\Delta\rho}{\rho} = \alpha\Delta T. \tag{22}$$

On the basis of a comparison to the Boussinesq problem at onset, it is generally assumed that $\alpha\Delta T < 0.2$ is an acceptable condition for B-ap to work. This criterion can be satisfied up to very high values of Ra (above 10^{15} for one set of data[55] and above 10^{16} for another[53]), although there is

no proof that asymmetries of this magnitude are without consequence at high Ra. In fact, a more stringent requirement of $\alpha \Delta T < 0.05$ was adopted by Niemela & Sreenivasan.[55]

At a speculative level, very close to the critical point, there may be some transient effects associated with compressibility, for instance a "piston effect" in heat transfer due to an adiabatic expansion which has well-understood effects near the onset of convection.[103,104] It is not clear whether this would lead to differences in the long-term turbulent state due to the boundary layers being regenerated continually (following plume emission) so that the normally transient piston effect could result in some effective steady state heat pumping.

Further empirical justification for thinking in terms of a critical point effect comes from recent experiments[65] in a container of reduced height and aspect ratio 4, in which anomalous heat transport enhancement (and increased scatter) were seen for the meager data obtained at operating points close to the critical temperature and pressure. Similar observations were reported earlier for aspect ratio unity[55] for the few points taken within the same range of the critical point but, notably, for much different values of the principal dynamical control parameter Ra.

Even away from the critical point there are confinement effects which tend to cloud the picture at moderate Rayleigh numbers. The corrections that have been formulated until now are parameterizations of empirical evidence which may or may not depend on subtleties of the experiments from which they are derived. For instance, the effect of partial heat propagation in the sidewall involves the complex interaction between a strong mean flow and the temperature distribution in the container. The mean flow may itself be a confinement effect that does not exist in laterally infinite systems,[65] and so it is not clear that we can "correct" it out of the problem. Also, since the mean flow may depend sensitively on boundary conditions, some subtle differences between experiments may have a greater overall effect on the resultant heat transport than we realize. Furthermore, considering that the large temperature gradients driving the convective flow occur at the walls—in the boundary layers—we should know better about the processes that occur there. A fuller knowledge of the stress at the wall as a function of Ra would put the global measurements of Nu in a substantially better light.

A principal disadvantage of low temperature helium gas experiments is that it has been difficult to measure the velocity directly. Clearly, knowledge of both velocity and temperature provides a better picture of the physics of turbulent convection.

3.3. Superfluid Turbulence

Under a set of assumptions that seem plausible, the root-mean-square superfluid vorticity has been measured. The assumptions, discussed in section 2.3.1, have to be put on firmer ground. Measurements of the root-mean-square value do not lead to the direct knowledge of the energy spectrum or the dynamics. For that, we would need to measure the velocity fluctuations. It is not clear how this can be done but we will consider a few possibilities in section 4.3. An interesting question is the local motion of the superfluid near the grid, and its possible influence on the decay dynamics. Experiments have shown that global averages of the superfluid line density decay are rather insensitive to the gross change in grids, although there is some small systematic difference. Within the framework we have discussed in section 2, the major issue needing explanation is the behavior of the effective kinematic viscosity of superfluid turbulence. A start in this direction has been made[16] and recent experiments[99] in ^{3}He-B have added important observations in the case where the effective kinematic viscosity has different values depending on whether one takes it as proportional to η_n/ρ or to κ. The correctness of the latter interpretation[16] has now been more firmly established.

4. PROSPECTS AND SUMMARY

4.1. Short Term Concerns

A promise of helium for classical turbulence research is that very high values of the control parameter such as the Reynolds and Rayleigh numbers can be obtained in relatively small apparatus, as can large ranges of these parameters. Our experience with the Kármán flow, thermal convection, as well as superfluid turbulence, has shown that this aspect of the promise has been realized. Indeed, new grounds have been broken in terms of the ranges of Reynolds and Rayleigh numbers attained.

The prospect of obtaining very high Re and Ra in apparatus of small physical size has imposed severe demands on instrumentation. The combination of small sizes of the apparatus (thus of the large scale) and high values of the control parameter leads to the generation of small scales that are physically very small (of the order of microns or less in existing experiments) and oscillate with frequencies on the order of MHz. Resolving these scales requires non-trivial development of small, fast, sensitive and durable probes. A few designs for temperature and velocity probes have been developed as discussed earlier, but their performance is less well understood than those of their room-temperature counterparts, and they seem to be subject to a larger number of limitations.

Because of this problem, we raise the issue that the promise of helium may not be easily realizable in its entirety. It is not clear to us that smaller probes based on the principles of the standard thermal anemometry are the solution to these problems, some of which arise because the use of helium elevated the Reynolds number of the probe itself to a higher level than in conventional fluids, leading to unfavorable heat transport characteristics.

In thermal convection flows, where some direct knowledge of the velocity would be most desirable even at scales much larger than the Kolmogorov scale, the use of hot and cold wires is made further complex by the fact that they require a steady flow—and the mean wind exists only near the boundaries and is also probably too weak to be effective. Also, there are both active temperature fluctuations in the cell and temperature fluctuations of the wire due the the velocity fluctuations that it is intended to measure. This particular limitation holds for room-temperature fluids as well.

Single-point measurements can also be made by using laser Doppler anemometry (LDA). The key to success is the proper tracer particles which follow the flow faithfully, so that a detection of their motion is the same as measuring the fluid velocity. One needs to seed the fluid with nearly buoyant tracer particles that can also scatter light effectively. The greater need is to measure the entire velocity field in a turbulent flow. Field measurements are more useful because turbulence consists of spatial structures of all sizes. To obtain an entire two-dimensional section of the turbulent flow field at a given instant in time, we may use the Particle Image Velocimetry (PIV).[105] Here, the fluid is typically illuminated by a laser sheet through some cross-section and the scattered light from the seeding particles is recorded by a camera at right angles to the plane of the light sheet. Two "exposures" separated by a small time increment are made, and local velocity vectors are obtained over the entire sheet area by (statistically) comparing the two exposures. Again, the key is the choice of the most suitable particles. This technique has, in fact, recently been applied in grid turbulence[85,106–108] at 4.2 K, as well as in counterflow turbulence[109] and in helium II turbulence.[110]

Liquid helium has a relatively low density and tiny hollow glass spheres have been used[85,108] for purposes of PIV. Beginning with Chopra & Brown[111] and Ichikawa & Murakami,[112] attempts have been made to inject hydrogen and solidify it into small particles. This work has been improved upon[109,110] recently. The use of hydrogen particles in helium II has been the latest step[110] in this direction, but more work is needed to make the technique routinely usable.

The seeding of helium gas for thermal convection experiments does not appear possible owing to the large variations and small values of the density, which at best is less than half that of the liquid phase. However, as mentioned already, liquid helium can also be used to attain high Ra; though this sacrifices the large range of Ra, we know that it can be seeded adequately. Considering the problems involved in de-convolving temperature and velocity fluctuations, the problems associated with gaining optical access and the limited range of Ra that one can attain, it is not clear that such an experiment ought be pursued without much thought.

Even so, it should be obvious that much can be gained from flow visualization in order to focus theoretical and experimental efforts, and yet this has not been well developed for cryogenic helium. It has a huge pay-off because most existing flow visualizations in water and other room-temperature fluids are at low to modest Rayleigh numbers, and the intuition that one derives from low Ra cannot readily be extended to high Ra. There are no intrinsic barriers to perfecting visualization tools—only that researchers are forced to develop both the technology and the science. This is not unique in scientific endeavor, but it slows down progress nonetheless. We may also remark that it is not easy to test new particles in the actual low temperature environment. In experimental phase, White[106] had resorted to testing in a pressurized SF_6 environment, where the density could be matched to that of liquid helium.

The selection of suitable tracer particles can indeed be helped by theory, especially in helium II. Recent theoretical work[113] addresses the behavior of particles in the simultaneous presence of the normal velocity, superfluid velocity and the vortex line velocity. Various regimes were found in which the tracer particles would either follow the motion of the superfluid, the normal fluid or the total mass current depending on the particle relaxation time. The relaxation time for the particularly simple case of neutrally buoyant particles is given by

$$\tau = \frac{\rho a_p^2}{3\mu_n}, \tag{23}$$

where a_p is the particle diameter, ρ the fluid density (here equal to particle density) and μ_n is the normal shear viscosity. Generally, when the eddy turnover time in turbulence is much smaller than the typical relaxation time given above, the particles will follow the total mass flow. If the opposite condition prevails, the particles will follow the normal fluid (at very low temperatures, however, the particles will follow the superfluid). It is thus clear that one must know the parameters of the tracer particles well in order to properly interpret the results of any measurement of their motion in helium II.

Where density gradients exist in the flow, visualization can occur in the absence of tracer particles, using shadowgraphs (which depend on density gradient) or the schlieren technique (which depends on the second derivative of the density). It has been demonstrated[114,115] that shadowgraphy can be used in helium I to visualize even weak flows near convective onset. A light beam reflected from the cell displays intensity variations resulting from convergence or divergence as a result of gradients in the refractive index. In the case of thermal convection, these gradients indicate the average temperature field. The signal is averaged over the fluid sample in the direction of light propagation, and so the technique does not give local information but only global features. In the case of large apparatus, installing an optically transparent but thermally conducting plates is a non-trivial task. For the case of turbulence under isothermal conditions, it would be possible to use helium 3 as a "marker" for shadowgraphs.

Scattering of ultrasound is another method that can, in principle, be used for velocity measurements in helium. It can be used in the gas phase which makes it a plausible candidate for cryogenic convection experiments. However, there would be substantial problems with achieving sufficiently high signal/noise resulting from a mismatch of acoustic impedance between sound transducers and helium. Much work along this direction has been performed[116,117] but no concrete results have come forth in turbulence.

4.2. Theoretical Issues

4.2.1. Continuum Approximation

An interesting question that has been raised at various times is whether the increasingly small scales in cryogenic helium flows render tenuous the continuum approximation of classical hydrodynamics. Even in the experiments already completed, does one have to worry about aspects of molecular motion? Frisch[118] has addressed this question in a general context and demonstrated that the ratio of the dissipation scale to the molecular mean free path *grows* with increasing Reynolds number. The hydrodynamic approximation thus becomes better applicable at higher *Re*.

Related to this interplay between microscopic and macroscopic degrees of freedom, though not focused on low temperature experiments, we note some previous attempts[119] to cast macroscopic observations in terms of molecular properties, in which case different working fluids could give rise to possibly measurable differences under otherwise similar conditions. Such assertions have not been substantiated by other measurements.[120] It appears highly plausible that the Navier-Stokes equations will remain the bedrock for the understanding of cryogenic turbulence as well.

4.2.2. Superfluid Turbulence

One of the subjects that derived resurgence from the recent helium measurements is superfluid turbulence. We have summarized the arguments of the hypothesis of coupled motion between the superfluid and classical turbulence. Under these conditions the superfluid turbulence behaves like classical turbulence with an effective kinematic viscosity which is of the same order as the kinematic viscosity of helium I. This important result puts to rest the notion that we may generate extremely large Reynolds numbers using helium II. Helium II flows will thus not be able to unlock qualitatively new understanding of classical turbulence through the attainment of fantastically high *Re* that were once thought possible. Even so, the increased understanding of the connection between the classical and superfluid fields of turbulence has been immensely rewarding. It is clear that superfluid turbulence on its own is an extremely important subject to study and understand.

4.3. Instrumentation Issues

As indicated above, the one single issue that has prevented greater progress from occurring is no doubt the inadequacy of suitable instrumentation. We list here a few possible avenues to pursue, without being exhaustive.

4.3.1. Direct Pressure Measurements

In the towed grid problem, it should be possible to use commercial piezo devices, such as used by Tabeling[34] in the Kármán flow. However, such devices would have to be towed behind the grid at various distances and the turbulence time decay data assembled from many runs, each with different transducer-grid separation distances. The interpretation will have to assume ergodicity to hold. Other possibilities utilizing MEMS technology to fashion miniature pressure transducers are being explored by Gary Ihas (Report of ICTP Workshop on Experimental Techniques for the Study of Superfluid Turbulence, in preparation).

4.3.2. Thermal Sensors for Boundary Layers

Development of thermal stress sensors for gaining information on the boundary layers will be particularly useful. However, the boundary layers can be quite small (of order $100\,\mu$m) at high *Ra* and hence micro-machining will be required.

4.3.3. Local Measurements

Many of the measurements, such as second sound scattering, measure global averages of the flow properties, while we want more detailed understanding of processes occurring over a small spatial scale. An attempt begun some years ago by Tabeling (personal communication) to develop a local second sound probe appears to have been abandoned. However, Roche and co-workers in Grenoble, as well as Skrbek in Prague, are continuing (Report of ICTP Workshop on Experimental Techniques for the Study of Superfluid Turbulence, in preparation) the development of miniature second sound detectors with dimensions as low as $300\,\mu$m.

4.4. Numerical Simulations

As we have hinted, the inherent difficulties of the Navier–Stokes equations have lead to a proliferation of phenomenology. In addition to the lack of suitable instrumentation, other factors have also limited progress. These factors in experiments include non-constant Prandtl number, the effect of imperfect boundary conditions, poor applicability of the B-ap in experiments, and so forth. Numerical work seems to provide some useful answers without these limitations, but it is beset with its own difficulties. The main difficulty is the large number of degrees of freedom in turbulence. In this connection, it is interesting to note that recent DNS[121] have been run up to $Ra = 2 \times 10^{14}$ for aspect ratio 1/2. In these simulations, Boussinesq conditions and constant $Pr = 0.7$ were strictly prescribed. Over nearly the last four decades of Ra an asymptotic Nu-Ra scaling range with log–log slope 1/3 was observed. It was further found that changes in the mean flow structure, including its cessation, occurred depending on the location of the dynamical operating point in the Ra-Pr phase space. The constant Pr of the simulation at high Ra is closest to the conditions of the experiment of Niemela et al.,[53] for which the average log Nu-log Ra slope was 0.32 (after taking into account the best estimates of corrections for the sidewall conductivity and finite conductivity of the top and bottom plates).

As in thermal turbulence, numerical simulations have helped us understand aspects of superfluid turbulence. Schwarz[122, 123] set the trend by using vortex methods and classical Euler hydrodynamics supplemented by certain algorithmic prescriptions for reconnection and boundary effects. His simulations were extended to various other flows but the common drawback of these simulations has been that they are kinematic. That is, the back reaction of the superfluid vorticity on the velocity field has not

been included and the velocity field had been imposed as given. This last issue has been amended recently,[124, 125] but those related to the reconnections and boundary effects have remained somewhat elusive. Since this issue is clearly quantum mechanical in nature, one has to go beyond the Navier–Stokes equations to address it correctly. Such efforts have indeed been made[126, 127] and the prescriptions used by Schwarz was found to be reasonable.

It should be emphasized that issues of grid resolution in numerical simulations have not been fully explored in these flows.

4.5. A Long-term Proposal for a Landmark Experiment

One of the excitements of helium turbulence has been the promise of a great turbulence experiment that will propel the subject to the level of importance and recognition that it deserves. The experiment on which a great deal of convergence has occurred is thermal convection. In order to improve contact with natural systems and to remain within the existing analytical framework, it is desirable to probe thermal turbulence in apparatus with large aspect ratios. Early attempts[52] to study large aspect ratio convection were limited to rather low Ra because of small absolute cell height, and therefore do not particularly apply to practical situations. In new experiments[65] in a container of aspect ratio 4, however, Rayleigh numbers of up to about 10^{13} have been achieved (with the last half-decade being regarded as too close to the critical point, as was briefly mentioned above in section 3.2). The main results of these experiments, within the B-ap, were that the heat transfer scaling exponent approached the "classical" value of 1/3 at high Ra from a slightly lower value of 0.31 at lower Ra. Some mean wind survived at low Ra and appeared to encompass the entire container, as it did for smaller aspect ratios. However, the long-time correlation between temperature sensors located in the path of the wind at the mid-height of the cell, but separated by a diameter, vanished in the region of power-law exponent 1/3. This observation is consistent with the global randomization of the bulk flow expected for the 1/3rd power law[60] to emerge, following the discussion in section 2.2.3. This is the first significant attempt to study high Ra turbulence in the RBC geometry that is closer to the theoretical discussion of section 2.2.3.

While this experiment has revealed considerable new information, the Rayleigh number it attains, without getting too close to the critical point, is about 5×10^{12}, which is many orders of magnitude below those relevant to geophysics and astrophysics. Clearly, to maintain large aspect ratio (4 being the minimum[128]) and also large height (to gain on Ra), one needs a physically tall and wide apparatus (say 2 m high and 8 m in diameter).

This will enable us to reach Rayleigh numbers of the order of 10^{18} with aspect ratio 4 (five orders of magnitude higher than is possible at present) well within the B-ap. Operating such a container will encounter many new difficulties in sealing and maintaining temperature homogeneity across the horizontal plates, but the returns would be immense for bringing a closure to the problem of thermal convection.

4.6. Final Remarks

Flow visualization and particle tracking have long been used in fluid dynamics to provide essential hints for theoretical efforts. As we have seen, there has been some experimental low temperature work in recent years involving PIV measurements in both helium I and II.[108,106,109,110] It is also clear from recent theoretical work[113] that the proper interpretation of observations requires some theoretical knowledge of the particle behavior.

Techniques based on seeded particles are unlikely to be of use in the type of turbulent convection experiments carried out, since they depend on using the gas phase for which suitable particles would be rather difficult to find. We note that the liquid phase also has favorable properties for obtaining high Ra, but it lacks the versatility of the gas phase in yielding large ranges of Ra. Even so, some flow visualization could be accomplished in a suitably designed optical cryostat at a reasonably high Ra, for which the Prandtl number would be nominally unity, as for the gas that is not too near the critical point.

Direct measurement of velocity by any means would be extremely useful. In principle, high frequency sound scattering can be used[116] but, as in optical methods, it is also easier in the liquid phase than in the gas phase. The traditional hot-wire method, as we have seen, has had some success and can be further adapted for low temperature use, but it is rather unlikely that this technique could be used in thermal convection studies, since the hot-wires require an adequately large mean background flow, and one must be able to separate temperature fluctuations from velocity fluctuations, since both lead to a similar wire response. While this is possible in principle, it appears that the effort needed is better devoted elsewhere.

A more speculative possibility is to attempt laser-induced fluorescence of metastable helium molecules, which can be used as the "tracer" particles for, say, a PIV measurement.[129] This could be a very sensitive tool with good spatial resolution (only molecules in the intersecting region of two crossed lasers would be excited to metastable states). It is also possible that a single molecule could be detected spectroscopically. Above 1 K, the molecules would likely move with the normal fluid component, allowing its velocity profile to be detected, provided that the molecules are not

trapped on vortex lines (Report of the ICTP Workshop on Experimental Techniques for the Study of Superfluid Turbulence, in preparation). Such a technique would be complementary to more typical second sound attenuation measurements.

Our overall understanding of thermal convection has increased slowly but steadily. At the highest Ra it is still not clear that we can disentangle effects of proximity to the critical point (section 3.2), particularly with respect to the reporting of an ultimate regime by some authors. Even if such enhanced heat transport may be related to a type of non-Boussinesq behavior associated with close approach to the critical point, one cannot rule out its existence at even higher Ra than presently possible,[53] if the critical point can be avoided. On the negative side, we should point out, however, that the ultimate regime has been rigorously ruled out in the limit of infinite Pr by Constantin & Doering[61] which would suggest that it might not appear at any other Pr as well.

This last statement notwithstanding (nature often has surprises in store) the most convincing test for an ultimate regime would be to devise[130] an experiment that can combine sufficiently large aspect ratio with high Ra, keep the Prandtl number constant and stay within Boussinesq conditions. Such an experiment is probably not without considerable technical difficulties. This large-scale low-temperature apparatus could be constructed, say at CERN or BNL, where there is an adequate refrigeration capacity. Having a horizontal dimension of several meters would require segmentation of the plates with multiplexing of the heating and temperature control. Fundamentally, this is no more complicated than the mirror arrays used in astrophysical observation[d]. The bottom plate with a constant heat flux condition has no structural limitations associated with its weight since it can be supported from below. The temperature controlled top plate would probably have some limitations in this respect. Estimates have been made of the cooling power required for a cell that is 5 m in diameter but also 10 m tall, and it is around 200 W at 4 K. This is not too severe. It is possible that, at the very high Ra attainable in such an apparatus, the mean wind becomes sufficiently weak even for low aspect ratio, thus recovering the situation in which flow confinement has a weak effect on the heat transport and other statistical properties of the flow. Any correction due to finite conductivity of the plates will be pushed to higher and higher Ra as the cell height is increased, and we can predict from scaling the observations in similar experiments that it will be

---

[d]Indeed, a similarly large experiment has recently been constructed for use with ambient air,[131] and such technological challenges have been met. However, because the fluid is air, the Rayleigh numbers reached are substantially lower than those aimed in the present context.

negligible for any helium experiment operated in the Boussinesq regime. Thus, even the small aspect ratio experiment at large height may present a qualitatively different system capable of adding new understanding of the problem of turbulent thermal convection.

In summary, one part of the promise of helium (namely large values and ranges of the control parameters) has been amply established; flows with huge values of Ra and Re have indeed been generated in laboratory-sized apparatus. However, the second part of the promise—of being able to develop versatile techniques for precise measurements of velocity and vorticity—has lagged behind substantially, despite some impressive gains. This aspect needs substantial investment. The third part of the promise, namely the possible use of superfluid helium to generate extremely high Reynolds numbers, has turned out to be impossible for reasons of principle.

ACKNOWLEDGMENTS

REFERENCES

1. D. J. Tritton, *Physical Fluid Dynamics.* Clarendon Press, Oxford (1988).
2. P. A. Davidson, *Turbulence: An Introduction for Scientists and Engineers.* Oxford University Press, Oxford (2004).
3. E. M. Spiegel, *Annu Rev. Astron. Astrophys.* **9**, 323 (1971).
4. G. A. Glatzmaier, R. C. Coe, L. Hongre, and P. H. Roberts, *Nature* **401**, 885 (1999).
5. G. Falkovich and K. R. Sreenivasan, *Phy. Today* **59**, 43 (2006).
6. M. P. Marder, *Condensed Matter Physics.* Wiley, New York (2000).
7. B. B. Mandelbrot, *Scientific Amer* **280**, 50 (1999).
8. National Research Council Report: *Condensed Matter and Materials Physics: Basic Research for Tomorrow's Technology*, 308 pages, National Academy Press (1999).
9. V. Yakhot and K. R. Sreenivasan, *J. Stat. Phys.* **121**, 823 (2005).
10. A. Oberbeck, *Annalen der Physik und Chemie* **7**, 271 (1879).
11. F. H. Busse, *Rep. Prog. Phys.* **41**, 1929 (1978).
12. A. N. Kolmogorov, *Dokl. Akad. Nauk SSSR* **30**, 9 (1941).
13. A. S. Monin and A. M. Yaglom, *Statistical Fluid Mechanics*, vol. 2, MIT Press, Cambridge, USA (1975).
14. K. R. Sreenivasan, *Phys. Fluids* **7**, 2778 (1995).
15. K. R. Sreenivasan and A. Bershadskii, *J. Fluid. Mech.* **554**, 477 (2006).
16. W. F. Vinen and J. J. Niemela, *J. Low Temp. Phys.* **128**, 167 (2002).
17. K. R. Sreenivasan and R. J. Donnelly, *Adv. Appl. Mech.* **37**, 239 (2001).
18. R. Verzicco, *Phys. Fluids* **16**, 1965 (2004).

19. E. Brown, A. Nikolaenko, D. Funfschilling and G. Ahlers, *Phys. Fluids* **17**, 075108 (2005).
20. J. Nikuradse, NASA TT F-10359 (1966). Translated from the German original *Forsch. Arb. Ing.-Wes.* No. 356 (1932).
21. C. J. Swanson, B. Julian, G. G. Ihas and R. J. Donnelly, *J. Fluid. Mech.* **461**, 51 (2002).
22. B. J. McKeon, C. J. Swanson, M. V. Zagarola, R. J. Donnelly and A. J. Smits, *J. Fluid Mech.* **511**, 41 (2004).
23. M. V. Zagarola and A. J. Smits, *Phys. Rev. Lett.* **78**, 239 (1997).
24. P. P. Craig and J. R. Pellam, *Phys. Rev.* **108**, 1109 (1957).
25. R. J. Donnelly (ed.), *High Reynolds Number Flows Using Liquid and Gaseous Helium*. Springer-Verlag, New York (1991).
26. J. C. Kaimal, J. C. Wyngaard, D. A. Hsugen, O. R. Cote, Y. Izumi, S. J. Caughey and C. J. Readings, *J. Atmos. Sci.* **33**, 2152 (1976).
27. R. A. Antonia, A. J. Chambers, S. Rajagopalan, K. R. Sreenivasan and C. A. Friehe, *J. Phys. Ocean.* **8**, 28 (1978).
28. K. R. Sreenivasan and B. Dhruva, *Prog. Theo. Phys. Suppl.* **130**, 103 (1998).
29. K. R. Sreenivasan, *Rev. Mod. Phys.* **71**, S383 (1999).
30. G. K. Batchelor, *The Theory of Homogeneous Turbulence*, Cambridge Univesity Press (1953).
31. K. R. Sreenivasan *Phys. Fluids* **27**, 1048 (1984).
32. K. R. Sreenivasan, *Phys. Fluids* **10**, 528 (1998).
33. Y. Kaneda, T. Ishihara, M. Yokakawa, M. Itakura and A. Uno, *Phys. Fluids* **15**, L21 (2003).
34. P. Tabeling, G. Zocchi, F. Belin, J. Maurer and H. Willaime, *Phys. Rev. E* **53**, 1613 (1996).
35. A. Arneodo, C. Baudet, F. Belin, R. Benzi, B. Castaing, B. Chabaud, R. Chavarria, S. Ciliberto, R. Camussi, F. Chilla, B. Dubrulle, Y. Gagne, B. Hebral, J. Herweijer, M. Marchand, J. Maurer, J. F. Muzy, A. Naert, A. Noullez, J. Peinke, F. Roux, P. Tabeling, W. van de Water and H. Willaime, *Europhys. Lett.* **34**, 411 (1996).
36. K. R. Sreenivasan and R. A. Antonia, *Annu. Rev. Fluid. Mech.* **29**, 435 (1997).
37. H. Tennekes and J. L. Lumley, *A First Course in Turbulence* MIT Press, Cambridge, Ma.(1971).
38. V. Emsellem, L. P. Kadanoff, D. Lohse, P. Tabeling and Z. Wang, *Phys. Rev. E* **55**, 2672 (1997).
39. P. Tabeling and H. Willaime, *Phys. Rev. E* **65**, 066301 (2002).
40. A. Gylfason, A. Ayyalasomayajula and Z. Warhaft, *J. Fluid Mech.* **501**, 213 (2004).
41. K. R. Sreenivasan and C. Meneveau *Phys. Rev. A* **38**, 6287 (1988).
42. G. Paladin and A. Vulpiani, *Phys. Rev. A* **35**, 1971 (1987).
43. K. R. Sreenivasan, *Flow Turbul Combust.* **72**, 115 (2004).
44. V. Yakhot and K. R. Sreenivasan, *Physica A* **343**, 147 (2004).
45. J. Schumacher, K. R. Sreenivasan and P. K. Yeung, *J. Fluid Mech.* **531**, 113 (2005).
46. J. Maurer and P. Tabeling, *Europhys. Lett*. **43**, 29 (1998).
47. A. Bezaguet, J. P. Dauvergne, S. Knoops, Ph. Lebrun, M. Pezzetti, O. Pirotte, J. L. Bret, B. Chabaud, G. Garde, C. Guttin, B. Hebral, S. Pietropinto, P. Roche, J. P. Barbier-Neyret, C. Baudet, Y. Gagne, C. Poulain, B. Castaing, Y. Ladam and F. Vittoz, *AIP Conference Proceedings* **613**, Cryogenic Engineering Conference, Madison, USA, 16-20/07/2001, 1399 (2002).
48. R. A. Antonia, B. R. Satyaprakash and A. K. M. F. Hussain, *J. Fluid Mech.* **119**, 55 (1982).
49. O. Chanal, B. Baguenard, O. Bethoux and B. Chabaud, *Rev. Sci. Instrum.* **68**, 2442 (1997).
50. D. C. Threlfall, *J. Fluid Mech.* **67**, 17 (1975).
51. B. Castaing, G. Gunaratne, F. Heslot, L. Kadanoff, A. Libchaber, S. Thomae, X.-Z. Wu, S. Zaleski and G. Zanetti, *J. Fluid Mech.* **204**, 1 (1989).

52. W.-Z. Wu, Ph.D. thesis, University of Chicago, Chicago (1991).
53. J. J. Niemela, L. Skrbek, K. R. Sreenivasan and R. J. Donnelly, *Nature* **404**, 837 (2000).
54. X. Chavanne, F. Chilla, B. Chabaud, B. Castaing and B. Hebral, *Phys. Fluids* **13**, 1300 (2001).
55. J. J. Niemela and K. R. Sreenivasan, *J. Fluid. Mech.* **481**, 355 (2003).
56. E. M. Sparrow, R. B. Husar and R. J. Goldstein, *J. Fluid Mech.* **41**, 793 (1970).
57. S. A. Theerthan and J. H. Arakeri, *J. FLuid Mech.* **373**, 221 (1998).
58. Y. B. Du and P. Tong, *J. Fluid Mech.* **407**, 57 (2000).
59. W. V. R. Malkus, *Proc. R. Soc. Lond. A* **225**, 196 (1954).
60. L. N. Howard, in *Proc. 11th Intern. Cong. Appl. Mech.,* H. Gortler (ed.), Springer, Berlin, p. 1109 (1966).
61. P. Constantin and C. R. Doering, *J. Stat. Phys.* **94**, 159 (1999).
62. R. H. Kraichnan, *Phys. Fluids* **5**, 1374 (1962).
63. D. Lohse and F. Toschi, *Phys. Rev. Lett.* **90**, 034502 (2003).
64. S. Grossmann and D. Lohse, *Phys. Rev. Lett.* **86**, 3316 (2001).
65. J. J. Niemela and K. R. Sreenivasan, *J. Fluid Mech.* **557**, 411 (2006).
66. P. Roche, B. Castaing, B. Chabaud, B. Hebral and J. Sommeria, *Euro. Phys. J.* **24**, 405 (2001).
67. G. Ahlers, *Phys. Rev. E.* **63**, 015303 (2001).
68. R. Verzicco, *J. Fluid Mech.* **473**, 201 (2002).
69. P. E. Roche, B. Castaing, B. Chabaud and B. Hebral, *J. Low Temp. Phys.* **134**, 1011 (2004).
70. J. J. Niemela, L. Skrbek, K. R. Sreenivasan and R. J. Donnelly, *J. Fluid Mech.* **449**, 169 (2001).
71. K. R. Sreenivasan, A. Bershadskii and J. J. Niemela, *Phys. Rev. E* **65**, 056306 (2002).
72. S. Cioni, S. Ciliberto and J. Sommeria *J. Fluid Mech.* **335**, 111 (1997).
73. X. L. Qui and P. Tong, *Phys. Rev. E* **64**, 036304 (2002).
74. E. Villermaux, *Phys. Rev. Lett.* **75**, 4618 (1995).
75. C. Sun, K.-Q. Xia, and P. Tong, *Phys. Rev. E* **72**, 026302 (2005).
76. E. Brown, A. Nikolaenko and G. Ahlers, *Phys. Rev. Lett.* **95**, 084503 (2005).
77. K. R. Sreenivasan, A. Bershadskii and J. J. Niemela, *Physica A* **340**, 574 (2004).
78. R. C. Hwa, C. B. Yang, S. Bershadskii, J. J. Niemela and K. R. Sreenivasan, *Phys. Rev. E* **72**, 066308 (2005).
79. A. Bershadskii, J. J. Niemela and K. R. Sreenivasan, *Phys. Lett. A* **331**, 15 (2004).
80. P. E. Roche, Ph.D. thesis, l'Universite Joseph Fourier (2001).
81. Y. B. Du and P. Tong, *Phys. Rev. Lett.* **81**, 987 (1998).
82. A. V. Gordeev, T. V. Chagovets, F. Soukoup and L. Skrbek *J. Low Temp. Phys.* **138**, 549 (2005).
83. A. P. Finne, T. Araki, R. Blaauwgeers, V. B. Eltsov, N. B. Kopnin, M. Krusius, L. Skrbek, M. Tsubota and G. E. Volovik, *Nature* **424** 1022 (2003).
84. V. S. L'vov, S. V. Nazarenko and G. E. Volovik *arXiv:nlin.CD/0408048 v3 3 Sep 2004*.
85. C. M. White, A. N. Karpetis and K. R. Sreenivasan, *J. Fluid Mech.* **452**, 189 (2002).
86. M. R. Smith, Ph.D. thesis, University of Oregon, Eugene (1992).
87. M. R. Smith, R. J. Donnelly, N. Goldenfeld and W. F. Vinen, *Phys. Rev. Lett.* **71**, 2583 (1993).
88. S. R. Stalp, Ph.D. thesis, University of Oregon, Eugene (1998).
89. J. J. Niemela, R. J. Donnelly and K. R. Sreenivasan, *J. Low Temp. Phys.* **138** 537 (2005).
90. C. F. Barenghi, S. Hulton and D. C. Samuels, *Phys. Rev. Lett.* **89,** 275301 (2002).
91. J. J. Niemela, L. Skrbek and S. Stalp in *Quantized Vortex Dynamics and Superfluid Turbulence* (Proceedings of a Workshop held at the Isaac Newton Mathematical Institute, August 2000), C. F. Barenghi, R. J. Donnelly and W. F. Vinen (eds.), Springer (2001).
92. C. F. Barenghi, R. J. Donnelly and W. F. Vinen, *J. Low Temp. Phys.* **52**, 189 (1983).
93. S. R. Stalp, J. J. Niemela, W. F. Vinen and R. J. Donnelly, *Phys. Fluids* **14**, 1377 (2002).

94. L. Skrbek and S. R. Stalp, *Phys. Fluids* **12**, 1997 (2000).
95. S. R. Stalp, L. Skrbek and R. J. Donnelly, *Phys. Rev. Lett.* **82**, 4831 (1999).
96. L. Skrbek, J. J. Niemela and R. J. Donnelly, *Phys. Rev. Lett.* **85**, 2973 (2000).
97. R. J. Donnelly, *Quantized Vortices in Helium II*. Cambridge University Press, Cambridge (1991).
98. D. Donzis, K. R. Sreenivasan and P. K. Yeung, *J. Fluid Mech.* **532**, 199 (2005).
99. D. I. Bradley, D. O. Clubb, S. N. Fisher, A. M. Guénault, R. P. Haley, C. J. Matthews, G. R. Pickett, V. Tselpin and K. Zaki *Phys. Rev. Lett* **96**, 035301 (2006).
100. J. Maurer and P. Tabeling, *Europhys. Lett.* **43**, 29 (1998).
101. S. Corrsin, in *Handbuch der Physik*, S. Flugge and C. Truesdell (eds.), Springer, Berlin, **8**, part 2, p. 524 (1963).
102. S. Grossmann and D. Lohse, *Phys. Lett. A* **174**, 449 (1993).
103. A. Furukawa and A. Onuki, *Phys. Rev. E* **66**, 016302 (2002).
104. H. Meyer and A. B. Kogan, *Phys. Rev. E* **66**, 056310 (2002).
105. M. Raffel, C. Willert and J. Kompenhaus, *Particle Image Velocimetry*, Springer, Berlin (1998).
106. C. M. White, Ph.D. thesis, Yale University, New Haven (2001).
107. R. J. Donnelly, A. N. Karpetis, J. J. Niemela, K. R. Sreenivasan, W. F. Vinen and C. M. White, *J. Low Temp. Phys.* **126**, 327 (2002).
108. A. N. Karpetis, C. M. White and K. R. Sreenivasan, *Phys. Rev. E* **62**, 4421 (2000).
109. T. Zhang and S. W. Van Sciver, *J. Low Temp. Phys.* **138**, 865 (2005).
110. G. P. Bewley, D. P. Lathrop and K. R. Sreenivasan, *Nature* **441**, 588 (2006).
111. K. L. Chopra and J. B. Brown *Phys. Rev.* **108**, 157 (1957).
112. N. Ichikawa and M. Murakami in *High Reynolds Number Flows Using Liquid and Gaseous Helium*, R. J. Donnelly (ed.), Springer-Verlag (1991).
113. D. R. Poole, C. F. Barenghi, Y. A. Sergeev and C. F. Vinen, *Phys. Rev. B* **71**, 064514 (2005).
114. A. L. Woodcraft, P. G. J. Lucas, R. G. Matley and W. Y. T. Wong, in *Proc. Intern. Workshop on Ultra-High Reynolds Number Flows*, R. J. Donnelly and K. R. Sreenivasan (eds.), Springer-Verlag p. 436 (1999).
115. R. G. Matley, W. Y. T. Wong, M. S. Thurlow, P. G. J. Lucas, M. J. Lees, O. J. Griffiths and A. L. Woodcraft, *Phys. Rev. E* **63**, 045301 (2001).
116. S. Siefer and V. Steinberg, *Phys. Fluids* **16**, 1587 (2004).
117. C. Baudet, S. Ciliberto and J.-F. Pinton, *Phys. Rev. Lett.* **67**, 193 (1991).
118. U. Frisch, *Turbulence: the Legacy of A. N. Kolmogorov*, Cambridge University Press (1995).
119. A. Muriel, S. Novopashin, J. Esguerra and E. Gutierrez, *Science Diliman* **11**, http://www.ovcrd.upd.edu.ph/vol%2011%20no2%20abs%201.htm
120. C. M. White and K. R. Sreenivasan, *Phys. Lett. A* **238**, 323 (1998).
121. G. Amati, K. Koal, F. Massaioli, K. R. Sreenivasan and R. Verzicco, *Phys. Fluids* **17**, 121710 (2005).
122. K. W. Schwarz, *Phys. Rev. B*, **31**, 5782 (1985).
123. K. W. Schwarz, *Phys. Rev. B*, **38**, 2398 (1988).
124. C. F. Barenghi, in *Quantized Vortex Dynamics and Superfluid Turbulence* C. F. Barenghi, R. J. Donnelly, W. F. Vinen (eds.), Springer, Berlin, pp. 4-14 (2001).
125. D. C. Samuels, in *Quantized Vortex Dynamics and Superfluid Turbulence*, C. F. Barenghi, R. J. Donnelly and W. F. Vinen (eds.), Springer, Berlin pp. 97-112, (2001).
126. J. Koplik and H. Levine, *Phys. Rev. Lett.* **71**, 1375 (1993).
127. C. Nore, M. Abid and M. E. Brachet, *Phys. Rev. Lett.* **78**, 3896 (1997).
128. R. M. Kerr, *J. Fluid Mech.* **419**, 325 (2000).
129. D. N. McKinsey, W. H. Lippincott, J. Nikkel and W. Rellergert, *arXiv:nucl-ex/0503006 v1 11 Mar 2005*.
130. J. J. Niemela, *J. Low Temp. Phys.* **134**, 447 (2004).
131. R. du Puits, C. Resagk, A. Tilgner, F. H. Busse and A. Thess "Structure of thermal boundary layers in turbulent Rayleigh Benard convection" (to be published in *J. Fluid Mech*).